

AD-A094 733

AIR FORCE INST OF TECH WRIGHT-PATTERSON AFB OH SCHOO--ETC F/8 1/2
TIME-CONSTRAINED MAXIMUM-ENERGY TURNS.(U)

DEC 80 S PETERSEN

UNCLASSIFIED

AFIT/6AE/AA/80D-17

NL

1 of 1
AD-A094 733

END
DATE
FILMED
3 81
DTIC

52

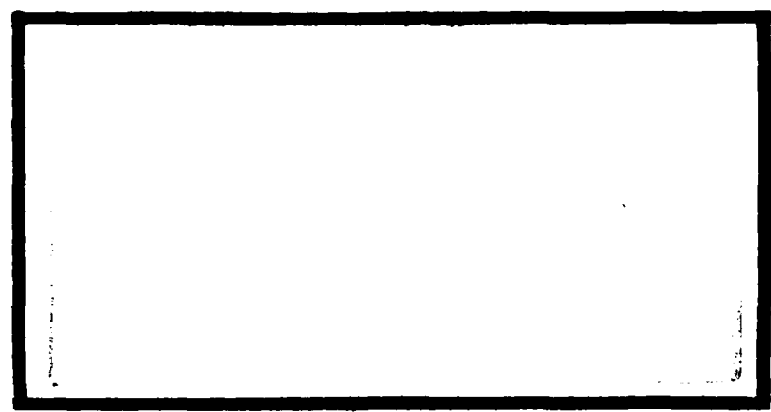
LEVEL ~~11~~

①

AD A094733



DTIC
SELECTED
FEB 9 1981
D
C



DAC FILE COPY

DEPARTMENT OF THE AIR FORCE
AIR UNIVERSITY (ATC)
AIR FORCE INSTITUTE OF TECHNOLOGY

Wright-Patterson Air Force Base, Ohio

DISTRIBUTION STATEMENT A
Approved for public release;
Distribution Unlimited

81 2 09 021

AFIT/GAE/AA/80D-17

23 JAN 1981
APPROVED FOR PUBLIC RELEASE AFR 190-17.

Laurel A. Lampela

LAUREL A. LAMPELA, 2Lt, USAF
Deputy Director, Public Affairs

Air Force Institute of Technology (AFIT)
Wright-Patterson AFB, OH 45433

TIME-CONSTRAINED MAXIMUM-ENERGY

TURNS

THESIS

AFIT/GAE/AA/80D-17 Steven Petersen
1Lt USAF

Approved for public release; distribution unlimited

TIME-CONSTRAINED MAXIMUM-ENERGY TURNS

THESIS

Presented to the Faculty of the School of Engineering
of the Air Force Institute of Technology
Air University
in Partial Fulfillment of the
Requirements for the Degree of
Master of Science

by
10 Steven/Petersen, B.S.
1Lt USAF
Graduate Aeronautical Engineering

December 1980

Approved for public release; distribution unlimited

1273

013

Acknowledgements

I would like to thank my thesis advisor, Captain James Rader, and my thesis committee of Captain James Silverthorn and Captain Robert Roach for their assistance and encouragement. I would also like to thank my good friend, Dr. R. Duke, for his moral support and encouragement. Finally, I would like to thank my wife, Peggy, for all her help and understanding during these 18 months.

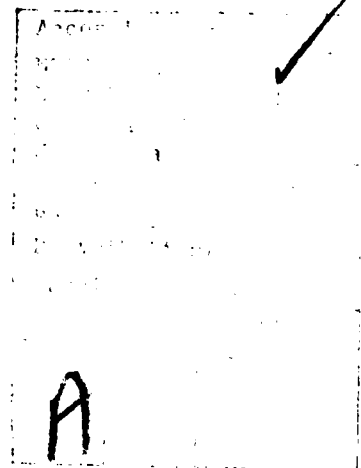


Table of Contents

	Page
Acknowledgements	ii
List of Figures	v
List of Tables	vi
List of Symbols	vii
Abstract	ix
I. Introduction	1
Background	1
Problem Statement	2
Assumptions	3
Approach	3
Summary of Current Knowledge	4
II. The Energy Turn Problem	5
Turn Conditions	5
Equations of Motion	5
Aerodynamic Forces	7
Thrust	8
Atmosphere	8
Control Constraints	9
III. Optimal Control Approach	10
Optimal Control Problem	10
Conditions to be Satisfied	11
Solving the Optimal Control Problem	12
IV. The Suboptimal Control Problem	13
Conditions to be Satisfied	13
Method of Solution	14
V. Solving the Constrained Energy Turn Problem	17
Equations of Motion	17
Control Variable Constraints	17
Control Variable Form	19
Numerical Methods	20
Convergence Factors	23
Control Evolution	23

VI.	Results	25
	Thrust Reversal	53
	Pilot Technique	53
VII.	Conclusions and Recommendations	55
	Bibliography	58
VITA	60

List of Figures

Figure	Page
1. K and C_{D_0} vs M	8
2. Angle of Attack vs Velocity	18
3. Roll Angle for Case 1 ($V_i=621$ ft/sec, $t=1.05t_{min}$) . .	30
4. Roll Angle for Case 2 ($V_i=621$ ft/sec, $t=1.10t_{min}$) . .	31
5. Roll Angle for Case 3 ($V_i=621$ ft/sec, $t=1.25t_{min}$) . .	32
6. Turn Plane for Case 1 ($V_i=621$ ft/sec, $t=1.05t_{min}$) . .	33
7. Turn Plane for Case 2 ($V_i=621$ ft/sec, $t=1.10t_{min}$) . .	34
8. Turn Plane for Case 3 ($V_i=621$ ft/sec, $t=1.25t_{min}$) . .	35
9. Energy Trajectories for the Low Speed Cases	36
10. Roll Angle for Case 4 ($V_i=903$ ft/sec, $t=1.05t_{min}$) . .	41
11. Roll Angle for Case 5 ($V_i=903$ ft/sec, $t=1.10t_{min}$) . .	42
12. Roll Angle for Case 6 ($V_i=903$ ft/sec, $t=1.25t_{min}$) . .	43
13. Turn Plane for Case 4 ($V_i=903$ ft/sec, $t=1.05t_{min}$) . .	44
14. Turn Plane for Case 5 ($V_i=903$ ft/sec, $t=1.10t_{min}$) . .	45
15. Turn Plane for Case 6 ($V_i=903$ ft/sec, $t=1.25t_{min}$) . .	46
16. Energy Trajectories for High Speed Cases 4, 5, and 6	47
17. Roll Angle for Case 7 ($V_i=903$ ft/sec, $t=1.05t_{min}$), and Case 8 ($V_i=903$ ft/sec, $t=1.10t_{min}$)	50
18. Turn Plane for Case 7 ($V_i=903$ ft/sec, $t=1.05t_{min}$), and Case 8 ($V_i=903$ ft/sec, $t=1.10t_{min}$)	51
19. Energy Trajectories for all High Speed Cases	52

List of Tables

Table	Page
1. Minimum Turning Times	4
2. Initial and Final Conditions	5
3. Compressibility Corrections	7
4. Optimal Coefficients for Case 1 ($V_i=621$ ft/sec, $t=1.05t_{\min}$)	27
5. Optimal Coefficients for Case 2 ($V_i=621$ ft/sec, $t=1.10t_{\min}$)	28
6. Optimal Coefficients for Case 3 ($V_i=621$ ft/sec, $t=1.25t_{\min}$)	29
7. Optimal Coefficients for Case 4 ($V_i=903$ ft/sec, $t=1.05t_{\min}$)	38
8. Optimal Coefficients for Case 5 ($V_i=903$ ft/sec, $t=1.10t_{\min}$)	39
9. Optimal Coefficients for Case 6 ($V_i=903$ ft/sec, $t=1.25t_{\min}$)	40
10. Optimal Coefficients for Cases 7 and 8 ($V_i=903$ ft/sec, $t=1.05t_{\min}$ and $1.10t_{\min}$)	49
11. Energy Summary	56

List of Symbols

x	- distance (x-direction)
y	- distance (y-direction)
h	- altitude
V	- velocity
θ	- flight path angle
ψ	- heading angle
S	- wing area
W	- weight
T	- thrust
L	- lift
D	- drag
N	- side force
ϵ	- thrust angle of attack
ζ	- thrust sideslip angle
ϕ	- bank angle
α	- angle of attack
π	- thrust control variable
g	- gravitational acceleration
g_0	- gravitational acceleration at sea level
ρ	- density
ρ_0	- density at sea level
σ	- density ratio
C_L	- lift coefficient
C_D	- drag coefficient

C_{L_α} - lift curve slope
 C_{D_0} - parasite drag coefficient
 K - induced drag parameter
 E - specific energy
 ΔE - change in specific energy
 G - performance index (E_f)
 F - augmented performance index
 X - state vector
 U - control vector
 M - final condition vector
 H - variational Hamiltonian
 λ - Lagrange multiplier vector (differential equations)
 v - Lagrange multiplier vector (final conditions)
 A - unknown parameter vector
 $()_i$ - initial value
 $()_f$ - final value
 $()_c$ - corner value
 $()_A - \frac{\partial ()}{\partial A}$ (A arbitrary)
 \dot{a} - $\frac{da}{dt}$ (a arbitrary)
 a^T - a transposed (a arbitrary)

Abstract

The object of this study is to find the trajectories which a high performance aircraft would employ to maximize the change in specific energy during a prescribed turn. These values of the change in specific energy are compared to the changes in specific energy which result from a minimum time turn. A suboptimal control approach, which uses both gradient and second-order parameter optimization techniques, is employed to find the maximum specific energy trajectories.

The results of the study show that turning times slightly greater than the minimum turning time allow large increases in aircraft specific energy, and that the trajectories can be flown with simple control inputs.

TIME-CONSTRAINED MAXIMUM-ENERGY TURNS

I Introduction

Background

Today's rapidly advancing technology has produced great improvements in fighter performance. Modern aircraft such as the F-15 and the F-16 have a thrust-to-weight ratio greater than one, and employ lightweight composites in some areas. These give the aircraft excellent maneuverability, far exceeding older aircraft such as the F-4 and the F-111. In light of this new capability, air combat tactics are being reviewed and modified so the pilot can take full advantage of the increased maneuverability. Aircraft modifications are also studied when further improvement may be possible.

Over the last decade the advantages and disadvantages of thrust reversal have been debated (Ref 1,2). The Navy tested a Grumman F-11 with an inflight thrust reverser and found that it could produce rapid accelerations and decelerations (Ref 3). However, they did not examine specific combat scenarios.

Johnson (Ref 4) studied minimum-time turns with thrust reversal. These 180 degree turns are common air combat maneuvers, and the pilot generally needs to turn as quickly as possible. Johnson found that thrust reversal could improve turning time, but the improvement was generally very small and could cost a great deal of aircraft specific energy. This

was a serious drawback, since specific energy is a measure of the aircraft's ability to engage and defeat opponents. One of Johnson's recommendations was to consider ways of conserving energy during a turn.

Problem Statement

The problem is finding the optimal controls that will maneuver a fighter aircraft through a given turn and enable the aircraft to gain the maximum energy. Turns are evaluated by taking slightly more time than the minimum and computing the controls. The minimum times were computed by Johnson (Ref 4). The simulation will include aircraft performance limits on thrust, angle-of-attack, and load factor.

The objective of the study is to determine whether a slightly longer turning time allows the aircraft to gain a significant amount of energy. A sufficiently large energy gain may well justify the longer turning time. If a large energy gain is obtained then an additional objective will be to determine simple tactics for flying the turn. The use of thrust reversal is not anticipated, but it is not specifically excluded.

The scope of this study is limited to finding the optimal trajectories and final energies starting from two different velocities and terminating at three sets of final conditions. Thus, six different cases are evaluated. The velocities are taken from previous work in order to make a meaningful comparison.

Assumptions

The following assumptions are made in order to model the equations of motion, the aerodynamic forces, and the atmosphere:

- a) the aircraft flies over a flat earth with constant gravity;
- b) all turns are coordinated;
- c) negligible fuel is consumed during the turn;
- d) thrust is collinear with velocity;
- e) errors introduced by small angle assumptions are negligible;
- f) lift is a linear function of angle of attack up to the angle of attack limit;
- g) maximum thrust is available throughout the turn;
- h) the atmosphere is modeled using the NASA standard atmosphere (Ref 5);
- i) the aircraft is initially in straight and level flight;
- j) controls are instantaneous.

These assumptions are identical to those employed in past studies (Ref 4,6). Thus, it is possible to compare results with these studies.

Approach

A specific turning situation is defined with initial and final conditions. The optimal control problem is defined and solution difficulties are explored. The problem is simplified by using a suboptimal control approach. This

approach is straightforward and has proved to be an effective means of computing the controls (Ref 6,7).

Summary of Current Knowledge

Johnson's minimum turning times for two sets of initial conditions are shown below. Neither case has reverse thrust capability.

Table 1. Minimum Turning Times

V_i (ft/sec)	h_i (ft)	E_i (ft)	V_f (ft/sec)	h_f (ft)	E_f (ft)	t_f (sec)
621	13990	19991	781	17350	26829	9.643
903	13990	26678	672	16150	23168	11.178

These results were obtained with the flight path angle and the heading angle initially equal to zero and final conditions of zero flight path angle and 180 degrees heading angle. The same initial and final conditions are used in this study in order to compare results.

II The Energy Turn Problem

The concept of the energy turn problem is to define trajectories which allow the aircraft to perform a specific turn and maximize the energy change

$$\Delta E = (E_f - E_i) = (h_f - h_i) + \frac{1}{2g}(v_f^2 - v_i^2) \quad (1)$$

during the turn. The turn is defined in terms of initial and final conditions. Then the equations of motion, aerodynamic forces, and atmosphere are specified.

Turn Conditions

The aircraft is assumed straight and level at the start of the turn. Initial and final conditions are summarized in Table 2, below:

Table 2. Initial and Final Conditions

CASE	V_i (ft/sec)	h_i (ft)	θ_i^0	ψ_i^0	θ_f^0	ψ_f^0	t_f	t_{min} (sec)
1	621	13990	0	0	0	180	$1.05t_{min}$	9.643
2	621	13990	0	0	0	180	$1.10t_{min}$	9.643
3	621	13990	0	0	0	180	$1.25t_{min}$	9.643
4	903	13990	0	0	0	180	$1.05t_{min}$	11.178
5	903	13990	0	0	0	180	$1.10t_{min}$	11.178
6	903	13990	0	0	0	180	$1.25t_{min}$	11.178

V is chosen below and above the corner velocity. The value of t_{min} is from Johnson's results (Ref 4).

Equations of Motion

During the turn the aircraft must obey the dynamic

equations of motion. Because trajectory analysis is concerned only with the development of the flight path, the aircraft can be modeled as a point mass. The equations of motion for a point mass aircraft over a flat earth as developed in Ref (8:48-49) are:

$$\dot{x} = V \cos \theta \cos \psi \quad (2)$$

$$\dot{y} = V \cos \theta \sin \psi \quad (3)$$

$$\dot{h} = V \sin \theta \quad (4)$$

$$\dot{V} = g \left(\frac{T}{W} \cos \epsilon \cos \zeta - \frac{D}{W} - \sin \theta \right) \quad (5)$$

$$\dot{\theta} = \frac{Q g \sin \phi}{W V} + \frac{g L \cos \phi}{W V} - \frac{g \cos \theta}{V} - \frac{T g}{W V} (\sin \phi \cos \epsilon \sin \zeta - \cos \phi \sin \epsilon) \quad (6)$$

$$\dot{\psi} = \frac{g \sin \phi}{V \cos \theta} \left(\frac{T}{W} \sin \phi + \frac{L}{W} \right) \quad (7)$$

Application of earlier assumptions yields $Q=0$, $\sin \zeta=0$, $\epsilon=\alpha$, $\sin \alpha=\alpha$, and $\cos \alpha=1$. The simplified equations are:

$$\dot{x} = V \cos \theta \cos \psi \quad (8)$$

$$\dot{y} = V \cos \theta \sin \psi \quad (9)$$

$$\dot{h} = V \sin \theta \quad (10)$$

$$\dot{V} = g \left(\frac{T}{W} - \frac{D}{W} - \sin \theta \right) \quad (11)$$

$$\dot{\theta} = \frac{g}{V} \left\{ \left(\frac{T}{W} \alpha + \frac{L}{W} \right) \cos \phi - \cos \theta \right\} \quad (12)$$

$$\dot{\psi} = \frac{g \sin \phi}{V \cos \theta} \left(\frac{T}{W} \alpha + \frac{L}{W} \right) \quad (13)$$

Aircraft motion is modeled with respect to an earth-fixed coordinate frame. The six state variables are x , y , h , V , θ , and ψ . The three control variables are α , ϕ , and T . The gravitational acceleration at 13990 ft is $g = 32.131 \text{ ft/sec}^2$ and is used throughout the turn. The aircraft weight is 12150 lbs. The aerodynamic forces, thrust, and atmosphere models appear in the sections that follow.

Aerodynamic Forces

These forces are composed of lift and drag. They are expressed as follows:

$$L = \frac{\rho_o \sigma V^2 S C_L}{2} \quad (14)$$

$$D = \frac{\rho_o \sigma V^2 S C_D}{2} \quad (15)$$

$$C_L = C_{L_\alpha} \alpha \quad (16)$$

$$C_D = C_{D_o} + K C_L^2 \quad (17)$$

For the aircraft modeled in this study, $S = 237 \text{ ft}^2$ and $C_{L_\alpha} = 5.0$ (Ref 4). Since flight in the transonic region is possible, compressibility corrections are made for K and C_{D_o} (Ref 9):

Table 3. Compressibility Corrections

M	K	C_{D_o}
0.0-.8	.05	.02
0.8-1.05	$.05 + .4(M-.8)$	$.02 + (M-.8)^2 \{6.016-5.12M\}$
1.05-1.25	$.05 + .4(M-.8)$	$.06 - .05(M-1.05)$

The corrections are approximate and are typical of this type of airfoil. Figure 1 depicts K and C_{D_0} vs M .

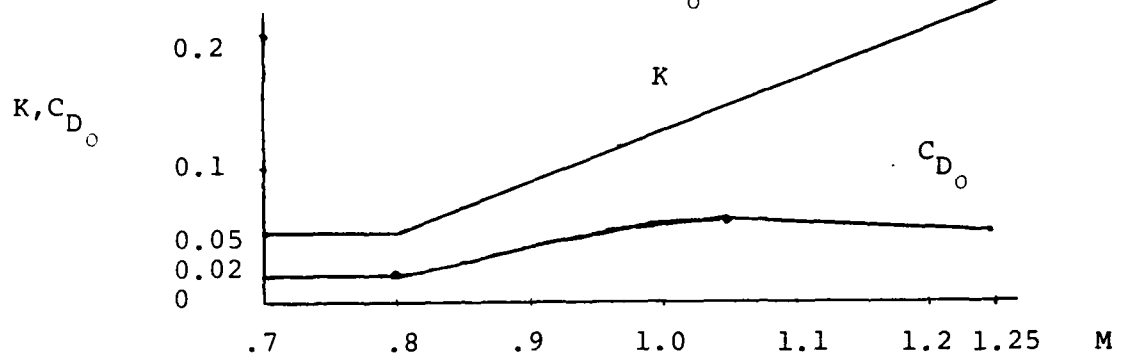


Figure 1. K and C_{D_0} vs M .

Thrust

It is assumed that maximum thrust is available throughout the turn. Thrust is given as

$$T = T_{\max} \pi, \quad (18)$$

where π is a thrust control variable. For constant weight the thrust to weight ratio becomes

$$\frac{T}{W} = \frac{T_{\max} \pi}{W} = \left(\frac{T}{W}\right)_{\max} \pi \quad (19)$$

For this aircraft the maximum thrust-to-weight ratio is 1.5.

Atmosphere

The density ratio σ in a standard atmosphere is defined (Ref 9) as

$$\sigma = \frac{\rho}{\rho_0} = \left\{ 1 - \left(\frac{n-1}{n} \right) \frac{g_0}{RT_0} h \right\}^{\frac{1}{n-1}} \quad (20)$$

The constants are:

$$\rho_0 = .002378 \text{ slugs/ft}^3$$

$$g_0 = 32.174 \text{ ft/sec}^2$$

$$T_0 = 518.688 \text{ deg R}$$

$$n = 1.235$$

$$R = 1715 \text{ ft}^2/\text{sec-deg R}$$

Control Constraints

There are three aircraft constraints. They are the angle of attack limit, the structural load limit, and the thrust limit:

$$\alpha_{\min} \leq \alpha \leq \alpha_{\max} \quad (21)$$

$$\frac{L}{W} \leq \left(\frac{L}{W}\right)_{\max} \quad (22)$$

$$T_{\min} \leq T \leq T_{\max} \quad (23)$$

or

$$\pi_{\min} \leq \pi \leq \pi_{\max} \quad (24)$$

The maximum lift-to-weight ratio for this aircraft is 7.22.

The maximum angle of attack is 0.2 radians.

III Optimal Control Approach

Classically, trajectory problems such as this are phrased in terms of an optimal control problem. This chapter defines the basic conditions that the optimal solution must satisfy.

Optimal Control Problem

The optimal control problem requires finding the functional relationships for the control variables that will maximize the aircraft specific energy. The energy is expressed as the performance index

$$G = h_f + \frac{V_f^2}{2g} \quad (25)$$

which is subject to the differential equations of motion

$$\dot{X} = f(X, u)$$

where X is the state vector and f represents the right side of eqns (8) through (13). The problem is further subject to the control constraints, eqns (21) through (24), and the initial and final conditions of Table 2. The final conditions are expressed as

$$M_1 = \theta_f \quad (26)$$

$$M_2 = \psi - 180. \quad (27)$$

When the final conditions are satisfied,

$$M = \begin{matrix} M_1 \\ M_2 \end{matrix} = 0. \quad (28)$$

Conditions to be Satisfied
(Ref {10:149-154})

The solution of the optimal control problem maximizes an augmented performance index, J , as

$$J = G + v^T M + \int_{t_i}^{t_f} \lambda^T (f - \dot{X}) dt \quad (29)$$

where v and λ are Lagrange multipliers. The variational Hamiltonian, H , is expressed as

$$H(X, u, \lambda) = \lambda^T f. \quad (30)$$

The optimal solution must satisfy the Euler-Lagrange equations:

$$\dot{\lambda} = -H_X^T = -\left(\frac{\partial H}{\partial X}\right)^T \quad (31)$$

$$\dot{X} = H_\lambda^T = \left(\frac{\partial H}{\partial \lambda}\right)^T \quad (32)$$

$$U_{opt} = \min_U H \quad (33)$$

The solution must also satisfy corner conditions and transversality conditions:

$$H_i = G_{t_i} = 0 \quad (34)$$

$$H_f + G_{t_f} = 0 \quad (35)$$

$$\lambda_i^T + G_{x_i} = 0 \quad (36)$$

$$\lambda_f^T - G_{x_f} = 0 \quad (37)$$

$$\Delta(H) - G_{t_c} = 0 \quad (38)$$

$$\Delta(\lambda^T) + G_{x_c} = 0 \quad (39)$$

$$G_v = 0 \quad (40)$$

Solving the Optimal Control Problem (Ref 11)

If the controls are neither on the boundaries nor singular, eqn (33) implies $H_u \approx 0$ which may be solved for the controls as functions of X and λ . Thus, the problem is converted to a boundary value problem. Initial values of λ are guessed, and the \dot{X} and $\dot{\lambda}$ equations are integrated. Generally, the end conditions are not satisfied. Various techniques can be used to vary the initial guesses, so that the end conditions (eqns (26), (27)) are satisfied.

One major problem with this method is guessing reasonable λ 's. This is difficult because the λ 's are not related to any physical quantities. Additionally, corners must be specified and this further complicates the problem. Hence, the boundary value problem is extremely difficult and time-consuming to solve. Since the problem is so difficult, the approach must be simplified so that a reasonable solution can be obtained. The Suboptimal Control Method is used to accomplish this.

IV The Suboptimal Control Problem

The suboptimal control problem is a parameter optimization problem. This transformation is achieved by assuming that the controls can be described by a known mathematical form, such as a polynomial, with coefficients represented by a vector A (Ref 4,6,7). Then the controls can be written as

$$U = U(t,A) \quad (41)$$

Equations (8) through (13) can be integrated from $t=0$ to $t=t_f$ and the final states will be functions of the A parameters:

$$X_f = X_f(A) \quad (42)$$

Hence, the performance index G and the final conditions M are also functions of A . The problem, then, is to find the A parameters which maximize the specific energy, G ,

$$G = G(A) \quad (43)$$

subject to the equations of motion

$$\dot{X} = f(X,A,t), \quad (44)$$

the final conditions

$$M(A) = 0, \quad (45)$$

and the control limits.

Conditions to be Satisfied

The augmented performance index, F , is defined as

$$F(A, v) = G(A) + v^T M(A) \quad (46)$$

Ordinary differential calculus requires an optimal set of A's and v's to satisfy 2 conditions:

$$F_A^T(A, v) = G_A + v^T M_A = 0 \quad (47)$$

$$F_v^T(A, v) = M(A) = 0 \quad (48)$$

where M_A and G_A are defined as

$$M_A = \frac{\partial M}{\partial A} \quad (49)$$

$$G_A = \frac{\partial G}{\partial A} \quad (50)$$

F_A represents a gradient that indicates the direction A should change to drive F_A to zero. F_A^T is a function of the A parameters. M is the final condition matrix which has two elements. A solution to the suboptimal control problem must only satisfy eqns (47) and (48). The v's can be computed with a gradient method (described in the next section), so the A coefficients are the only values which must be guessed. These are the controls and are easy to guess since they directly relate to physical quantities. The optimal control problem requires one to guess λ 's, which are unrelated to physical quantities and are very difficult to guess. Thus, the sub-optimal approach is much simpler to implement than the optimal control approach.

Method of Solution

Hull and Edgeman define a second order parameter

optimization technique in Ref 7. This technique is designed specifically for suboptimal control problems and is employed here. The method uses second order information to change the A parameters and the Lagrange multipliers v such that F_A and M are driven to zero (eqns (47) and (48)). Changes to A and v are computed as follows:

$$\delta v = (M_A F_{AA}^{-1} M_A^T)^{-1} (-P M_A F_{AA}^{-1} F_A^T + Q M) \quad (51)$$

$$\delta A = -F_{AA}^{-1} (P F_A^T + M_A^T \delta v) \quad (52)$$

where

$$F_{AA} = \frac{\partial^2 F}{\partial A^2} = G_{AA} + v_1 M_{AA1} + v_2 M_{AA2}. \quad (53)$$

P and Q are scaling factors that control optimization and end condition satisfaction, while F_{AA} contains second order information. The iterative algorithm for the method is:

1. guess v and A
2. integrate the equations of motion to find X
3. compute M , M_A , M_{AA} , G_A , and G_{AA}
4. select values of P and Q
5. compute values of δv and δA
6. compute $v = v + \delta v$ and $A = A + \delta A$
7. check for convergence and go to step 2 if not converged.

Convergence is obtained when each F_A term and each M are less than some small tolerance. The initial vector v is computed using relationships which were developed by Hull and Edgeman:

$$v = (M_A M_A^T)^{-1} \{ (Q/P)M - M_A G_A^T \} \quad (54)$$

$$\delta A = -P F_A^T \quad (55)$$

One characteristic of the second-order method is that it requires very good initial guesses. Usually the first-order method is used until the changes in v and A become very small. Then, the second-order method is employed (Ref 4,7).

The only real difficulty with the suboptimal control approach involves the selection of the scaling factors P and Q . This is explained in section V.

V Solving the Constrained Energy Turn Problem

The energy turn problem must be solved with numerical methods. Here, the energy turn problem, defined in chapter II, is adapted to the suboptimal control method. This chapter presents the actual forms of the equations of motion, control constraints, numerical derivatives, and convergence criteria.

Equations of Motion

The equations of motion are represented by eqns (8) through (13). Substitutions for the aerodynamic, atmospheric, and gravitational parameters yield the following equations:

$$\frac{dx}{dt} = V \cos \theta \cos \psi \quad (56)$$

$$\frac{dy}{dt} = V \cos \theta \sin \psi \quad (57)$$

$$\frac{dh}{dt} = V \sin \theta \quad (58)$$

$$\frac{dV}{dt} = 48.20\pi - V^2(D/12150) - 32.13 \sin \theta \quad (59)$$

$$\frac{d\theta}{dt} = \frac{32.13}{V} \{ (1.5\pi\alpha + (L/12159)) \cos \phi - \cos \theta \} \quad (60)$$

$$\frac{d\psi}{dt} = \frac{32.13}{V} (1.5\pi\alpha + (L/12150)) \quad (61)$$

Control Variable Constraints

Two of the three controls are affected by constraints. The thrust parameter has a maximum value of 1, so that

$$0 \leq \pi \leq 1 \quad (62)$$

Equations (21) and (22) each define a constraint on the angle of attack. For the load factor,

$$\frac{\rho_0 \sigma V^2 S C_{L_\alpha}}{2W} \leq \left(\frac{L}{W}\right)_{\max} \quad (63)$$

The load factor constraint can be simplified to

$$\sigma V^2 \alpha \leq 62060.6 \quad (64)$$

The angle of attack constraint is

$$\alpha \leq .2 \quad (65)$$

These constraints are illustrated in Figure 2.

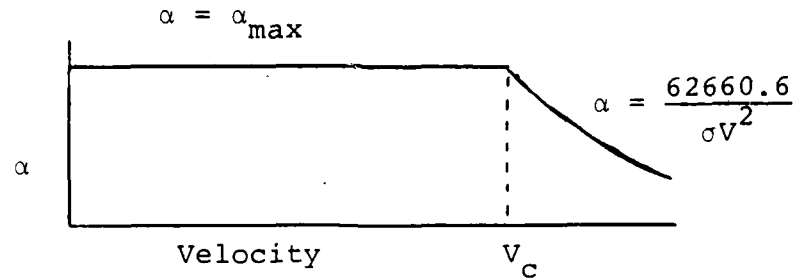


Figure 2. Angle of Attack vs Velocity

The corner velocity V_c is the velocity at which the lift coefficient for flight at the maximum load factor is the maximum lift coefficient. The corner velocity can be specified as

$$V_c = \left(\frac{62660.6}{\alpha_{\max} \sigma} \right)^{\frac{1}{2}} \quad (66)$$

Using eqn (65) for α_{\max} yields

$$V_c = 559.735 \sigma^{-\frac{1}{2}} \quad (67)$$

Control Variable Form

The controls were represented by a series of Chebyshev polynomials. These polynomials were selected because of good numerical behavior over the control ranges (Ref 8). The polynomials, $T_i(t)$, are functions of time. For $i=1$ to $i=6$ they are as follows:

$$T_1(t) = 1 \quad (68)$$

$$T_2(t) = 2t - 1 \quad (69)$$

$$T_3(t) = 8t^2 - 8t + 1 \quad (70)$$

$$T_4(t) = 32t^3 - 48t^2 + 18t - 1 \quad (71)$$

$$T_5(t) = 128t^4 - 256t^3 + 160t^2 - 32t + 1 \quad (72)$$

$$T_6(t) = 512t^5 - 1280t^4 + 1120t^3 - 400t^2 + 50t - 1 \quad (73)$$

The control variables are then

$$\phi(t) = \sum_{k=1}^{NPH} B_k T_k(t) \quad (74)$$

$$\pi(t) = \sum_{m=1}^{NPI} C_m T_m(t) \quad (75)$$

$$\alpha(t) = \sum_{n=1}^{NA} D_n T_n(t) \quad (76)$$

where B , C , and D are the unknown coefficients; NPH , NPI , and NA are the numbers of unknown coefficients; and ϕ , π , and α are the corresponding controls.

The constraints are exercised in the program by limiting

the value of each control to its known maximum or minimum whenever the polynomial would require it to exceed those limits. During the integration the controls are continually checked to determine if they are moving onto or off of a boundary. If so, the integration stepsize is adjusted so that the integration stops and starts again when the controls intersect the boundaries. In this manner the accuracy is preserved. This is especially important for the α limits.

Under certain conditions the π and α controls will not be parameters in the problem. This situation is best illustrated by the case in which all the controls are constant. If π and/or α are at their maximum values and if the F_A 's for these controls are negative, then in order to change the controls so the F_A 's are driven to zero, the controls must exceed their maximum value. Likewise, if either control is at its minimum and the corresponding F_A is positive, then the control must go below its minimum value. In either case, the coefficients no longer become parameters because they are fixed at their limits and their F_A terms cannot be driven to zero. Thus, the effects of these coefficients must be eliminated in order to calculate δv and δA without their influence. This is accomplished by dropping these parameters from the matrices used to calculate δv and δA (Ref 4).

Numerical Methods

The algorithm requires the matrices M , M_A , M_{AA} , G_A , and G_{AA} . M is evaluated by integrating the equations of motion to yield the final states. A fifth-order, Runge-Kutta,

controllable step size integration technique employing Fehlberg coefficients is used (Ref 13). The variable step size provision allows the technique to limit truncation error and makes it more accurate than fixed-step methods.

The M_A , M_{AA} , G_A , and G_{AA} matrices are determined by using a central difference numerical derivative technique (Ref 14). The equations of motion integrated using a positively perturbed A_n

$$A_{n+} = A_n + \delta n \quad (77)$$

and a negatively perturbed A_n

$$A_{n-} = A_n - \delta n \quad (78)$$

with δn as some small value. This yields M_+ , M_- , G_+ , and G_- . M_A and G_A are computed as

$$M_A = \frac{M_+ - M_-}{2\delta n} + \sigma(\delta^2 n) \quad (79)$$

$$G_A = \frac{G_+ - G_-}{2\delta n} + \sigma(\delta^2 n) \quad (80)$$

where $\delta^2 n$ is the error term. The M_A matrix contains two rows. The first row is determined by substituting M values from eqn (26) into eqn (90). The second row comes from eqn (27) and eqn (90). The two M_{AA} matrices and the G_{AA} matrix are obtained using a similar technique. Two parameters A_n and A_m are each perturbed both ways so that M_{++} , M_{--} , M_{+-} , M_{-+} , G_{++} , G_{--} , G_{+-} , and G_{-+} are obtained. The central difference representations for the second derivatives are:

$$M_{A_n A_m} = \frac{M_+ - 2M + M_-}{\delta n^2} + \sigma(\delta^2 n) \quad (81)$$

and

$$G_{A_n A_m} = \frac{G_+ - 2G + G_-}{\delta n^2} + \sigma(\delta^2 n) \quad (82)$$

if $n = m$, and

$$M_{A_n A_m} = \frac{M_{++} - M_{+-} - M_{-+} + M_{--}}{4\delta n \delta m} + \sigma(\delta n \delta m) \quad (83)$$

and

$$G_{A_n A_m} = \frac{G_{++} - G_{+-} - G_{-+} + G_{--}}{4\delta n \delta m} + \sigma(\delta n \delta m) \quad (84)$$

when $n \neq m$. As before, the M_{AA} matrices are formed by using eqn (26) values for the first matrix and eqn (27) values for the second matrix.

The error terms can be ignored for sufficiently small δn 's. δn is computed as

$$\delta n = \xi(A_n); \quad (85)$$

however, if the absolute value of δn is smaller than ξ , then

$$\delta n = \xi \quad (86)$$

where ξ is a small positive number. Various ξ values were tried in preliminary calculations in order to determine an accurate one. It was found that

$$\xi = 0.002 \quad (87)$$

gave consistent, accurate results.

Convergence Factors

The P and Q factors control optimization and end condition satisfaction, respectively. These factors are used to determine the size of δv and δA for each iteration. If the δ 's are too large, the method will miss $F_A=0$ and $M=0$. If the δ 's are too small, truncation error will cause the method to wander, again missing the solution. A variety of procedures can be devised to vary P and Q, but δv and δA must fall in a linear region about the nominal values. For the energy turn problem the algorithm was started with $Q=1$. This allowed the algorithm to quickly match the end conditions. P was slowly raised as the F_A terms decreased. The best end conditions and performance index are obtained when $Q=P=1$ (Ref 7). Initially the gradient method was used. When it became inefficient the second-order method was employed. The method was stopped when $P=1$ and the following conditions were satisfied:

$$M \leq 10^{-4} \quad (88)$$

$$F_A \leq 10^{-4} \quad (89)$$

Excluded were F_A terms related to boundary controls, since these terms can not be driven to zero.

Control Evolution

The trajectory evaluation was started by using constant controls for the bank, thrust, and angle of attack. The iteration procedure was followed until the solution satisfied eqns (88) and (89). Then another bank angle coefficient was included and another solution was computed, with bank as a

linear function of time. The bank coefficients were continually increased in this manner until the additional coefficient had little effect on the performance index. Finally, ways of improving the other controls were studied.

This approach to the controls was used on the six cases described in Table 2. The first three cases start from $V_i = 621$ ft/sec with the final time equal to 105%, 110%, and 125% of the minimum turning time, respectively. The second three cases start from $V_i = 903$ ft/sec with the final time equal to 105%, 110%, and 125% of the minimum turning time, respectively. Trajectories were computed for these six cases, and then the thrust controls were modified for the high speed cases of 105% and 110%. These results are presented in the next chapter.

VI Results

The trajectories that have been obtained show that a moderate increase in turning time can increase the specific energy. In some cases the increases are quite large.

The best gains occur for the high speed cases, with $V_i = 903$ ft/sec. When performing a minimum time turn one tries to decelerate to the corner velocity, since the turn rate is highest at that velocity. In Johnson's study, this deceleration caused a large loss of energy (Ref 4). By increasing the turning time, one allows a slower turn rate, which then permits a higher aircraft velocity. Thus, less deceleration is required and the final velocity and specific energy are higher. As each case was solved the effects of each control became apparent.

The thrust control adds energy to the aircraft. This energy can be used to increase velocity, altitude, or some combination of both. One would anticipate that the highest energy gains would utilize maximum throttle, and this was proved true. Cases 1, 2, 3, and 6 had a full throttle ($\pi=1$) in their final trajectories.

The angle of attack control determines the turn rate and the climb rate. Johnson (Ref 4) found that $\alpha=\alpha_{\max}$ gave the highest turn rate, and that lower α 's required longer to turn the aircraft. In cases where the turning time is quite short ($1.05t_{\min}$) a full α_{\max} is required in order to satisfy the end conditions. In cases 2 and 3 the turning time is large enough

so that α is less than α_{\max} for a portion of the turn.

The bank angle ϕ matched the thrust to the turn rate so that end conditions would be satisfied. It also establishes the plane of the turning trajectory. The results show the turn is performed in a constant plane in three-dimensional space. This plane is inclined to the y-axis and includes the x-axis. Thus, a graph of crossrange y versus altitude h shows the trajectories as essentially straight lines (Figs 13-15). For the high speed cases the planes became more vertical as the number of bank coefficients was increased, illustrating altitude gains from one solution to the next.

The optimal coefficients for the polynomial controls of cases 1, 2, and 3 are shown in Tables 4, 5, and 6. As the bank control is increased in complexity the performance index increases. However, above linear forms the additional bank coefficients do not add a large amount of energy. The controls are computed for constant, linear, quadratic, and cubic roll functions while holding thrust and angle of attack constant. The roll control histories for the low speed cases are shown in Fig 3 through Fig 5. Crossrange plots for each case are in Fig 6 through Fig 8. Figure 9 shows the final energy trajectory for each case on a velocity-altitude graph. As the graph shows, the specific energy does rise dramatically from one case to the next. This graph can be related to past studies of energy maneuvers.

Rutowski studied minimum time energy climbs in his paper on aircraft performance (Ref 15). He found that for a pure

TABLE 4

OPTIMAL COEFFICIENTS FOR CASE 1 ($V_i = 621$ ft/sec, $t = 1.05 t_{\min}$)

		CONSTANT	LINEAR	QUADRATIC	CUBIC
FINAL ENERGY	E_f	.257383E+05	.277946E+05	.277973E+05	.278018E+05
BANK ANGLE COEFF.	B_1	.143161E+01	.144944E+01	.146872E+01	.147017E+01
	B_2		.436564E+00	.455637E+00	.407126E+00
	B_3			.513851E-01	.546349E-01
	B_4				-.648807E-01
THRUST COEFF.	C_1	.820299E+00	.100000E+01	.100000E+01	.100000E+01
ANGLE OF ATTACK COEFF.	D_1	$\alpha = .2$ if $V < V_c$, $\alpha = (62060.6/V^2)$ if $V > V_c$			
LAGRANGE MULT.	v_1	-.131733E-01	.953453E-01	.982450E-01	.982189E-01
	v_2	-.317588E+00	-.282669E+00	-.284569E+00	-.284026E+00

TABLE 5

OPTIMAL COEFFICIENTS FOR CASE 2 ($V_i = 621$ ft/sec, $t = 1.10 t_{\min}$)

		CONSTANT	LINEAR	QUADRATIC	CUBIC
FINAL ENERGY	E_f	.281682E+05	.283677E+05	.283802E+05	.283840E+05
BANK ANGLE COEFF.	B_1	.143315E+01	.143851E+01	.149074E+01	.148989E+01
	B_2		.430340E+00	.481643E+00	.438371E+00
	B_3			.137070E+00	.136044E+00
	B_4				-.756511E-01
THRUST COEFF.	C_1	.999922E+00	.100000E+01	.100000E+01	.100000E+01
ANGLE OF ATTACK COEFF. *	D_1	.200000E+00	.180645E+00	.180720E+00	.179956E+00
LAGRANGE MULT.	v_1	.139104E+00	.115096E+00	.122628E+00	.123621E+00
	v_2	-.208522E+00	-.236112E+00	-.242374E+00	-.242720E+00

*: When $V > V_c$, $\alpha = (62060.6/V^2)$.

TABLE 6

OPTIMAL COEFFICIENTS FOR CASE 3 ($V_i=621$ ft/sec, $t=1.25t_{\min}$)

		CONSTANT	LINEAR	QUADRATIC	CUBIC
FINAL ENERGY	E_f	.292500E+05	.300272E+05	.300527E+05	.300668E+05
BANK ANGLE COEFF.	B_1	.142079E+01	.138822E+01	.147622E+01	.147669E+01
	B_2		.878277E+00	.880551E+00	.799804E+00
	B_3			.209266E+00	.221094E+00
	B_4				-.148614E+00
THRUST COEFF.	C_1	.100000E+01	.100000E+01	.100000E+01	.100000E+01
ANGLE OF ATTACK COEFF. *	D_1	.148058E+00	.148227E+00	.147443E+00	.147289E+00
LAGRANGE MULT.	v_1	.283761E+00	.160912E+00	.177088E+00	.170733E+00
	v_2	-.101059E+00	-.183663E+00	-.183058E+00	-.180346E+00

*: When $V > V_c$, $\alpha = (62060.6/V^2)$.

CASE 1

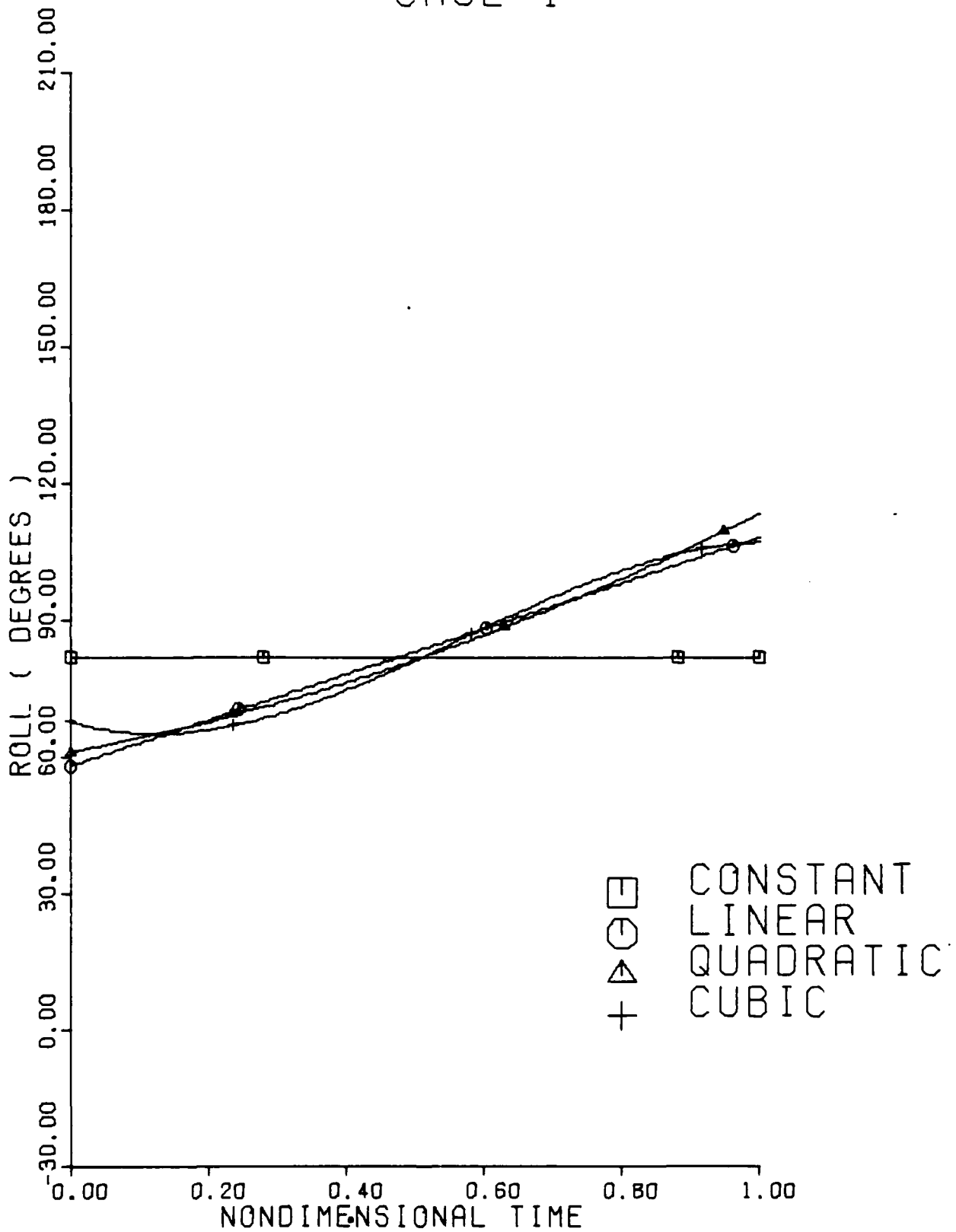


Figure 3. Roll Angle for Case 1 ($V_i=621$ ft/sec, $t=1.05t_{min}$)

CASE 2

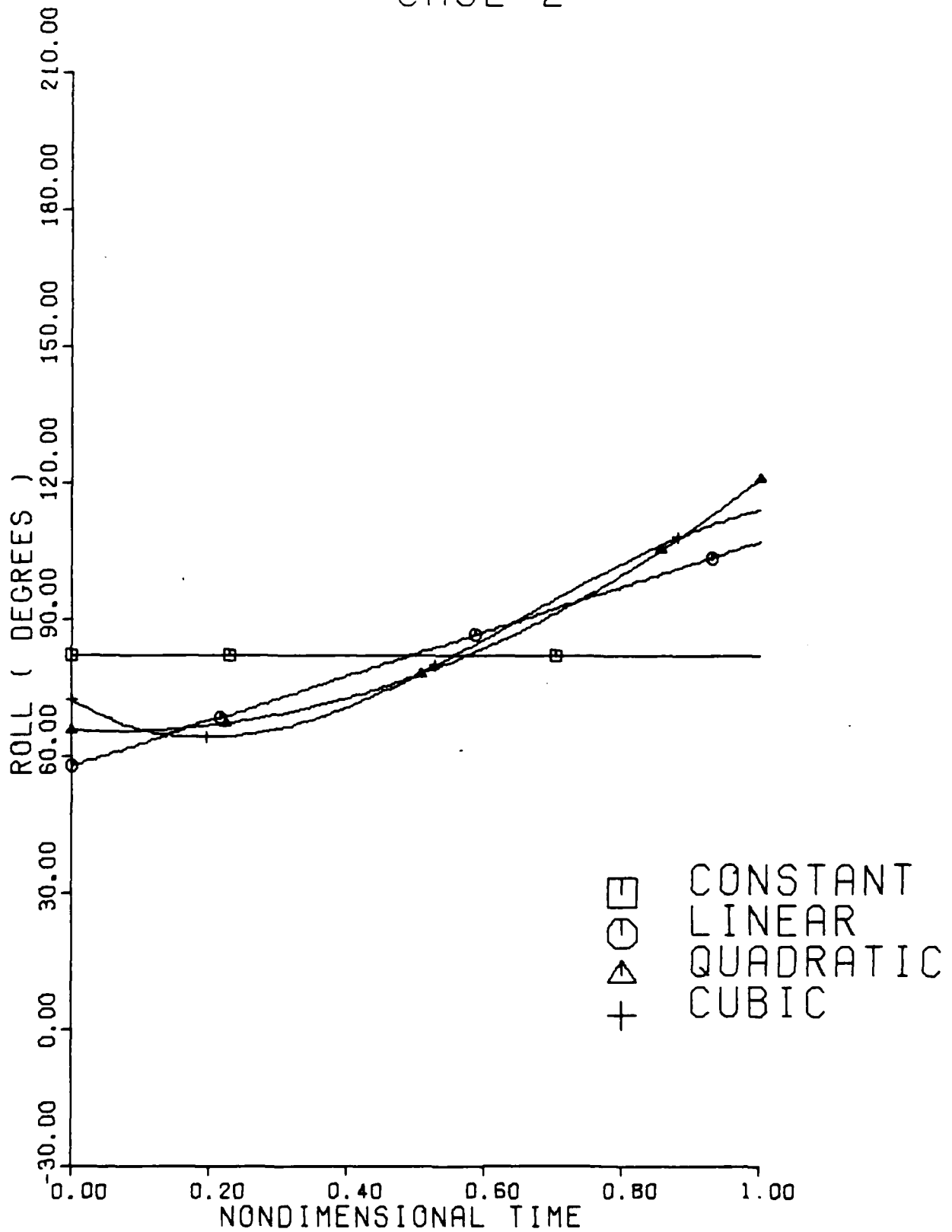


Figure 4. Roll Angle for Case 2 ($V_i = 621$ ft/sec, $t = 1.10t_{\min}$)

CASE 3

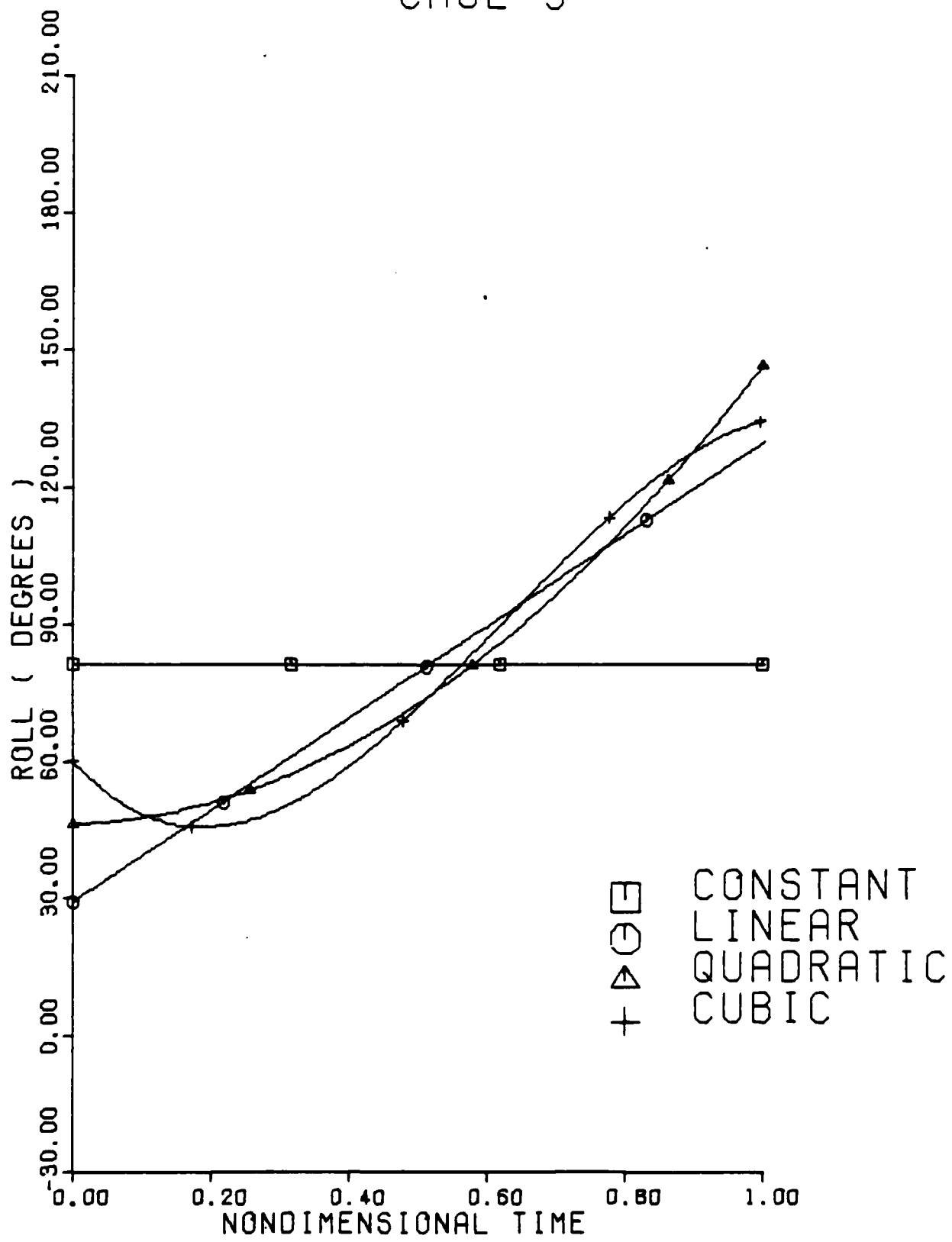


Figure 5. Roll Angle for Case 3 ($V_i=621$ ft/sec, $t=1.25t_{min}$)

CASE 1

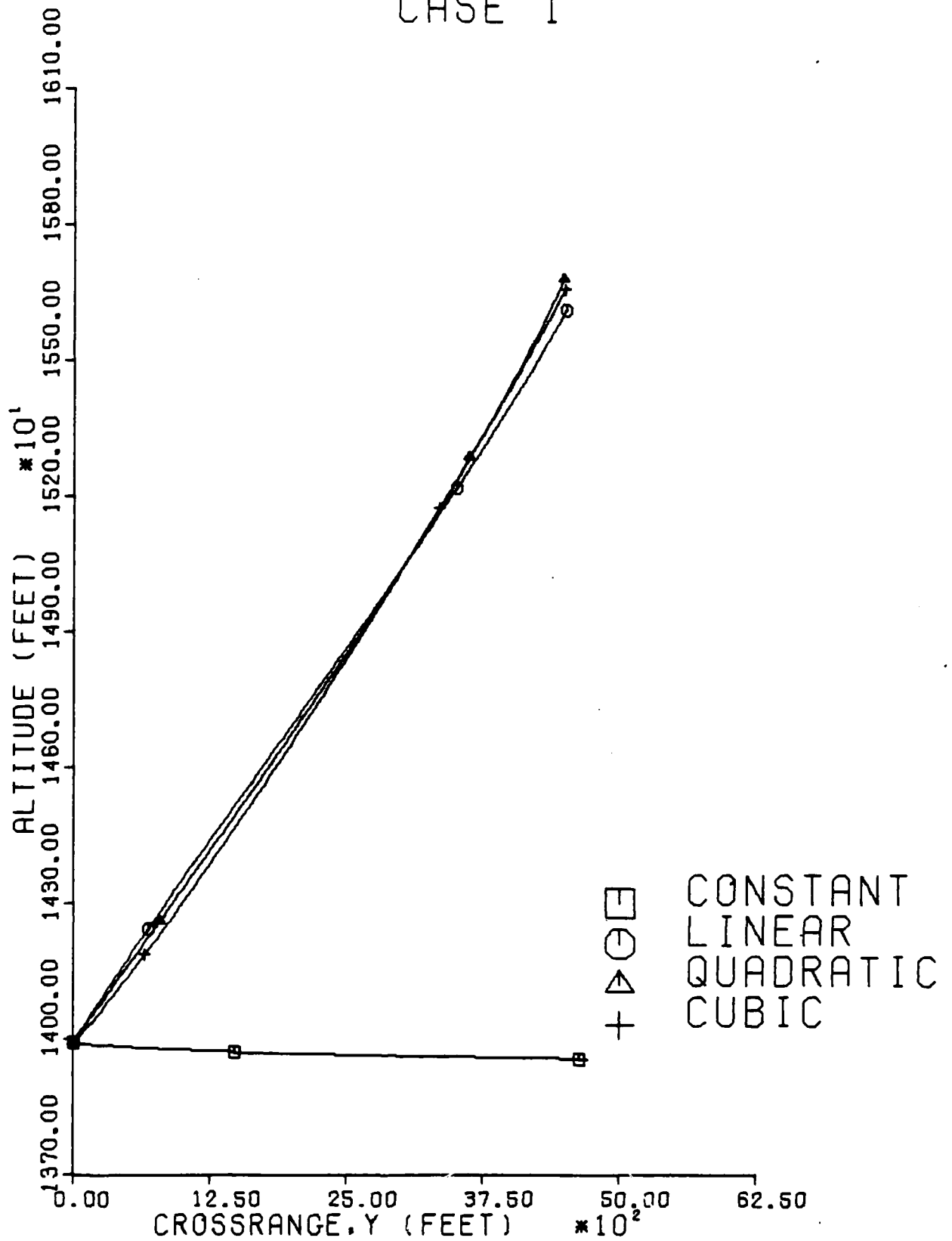


Figure 6. Turn Plane for Case 1 ($V_i=621$ ft/sec, $\tau=1.05t_{\min}$)

CASE 2

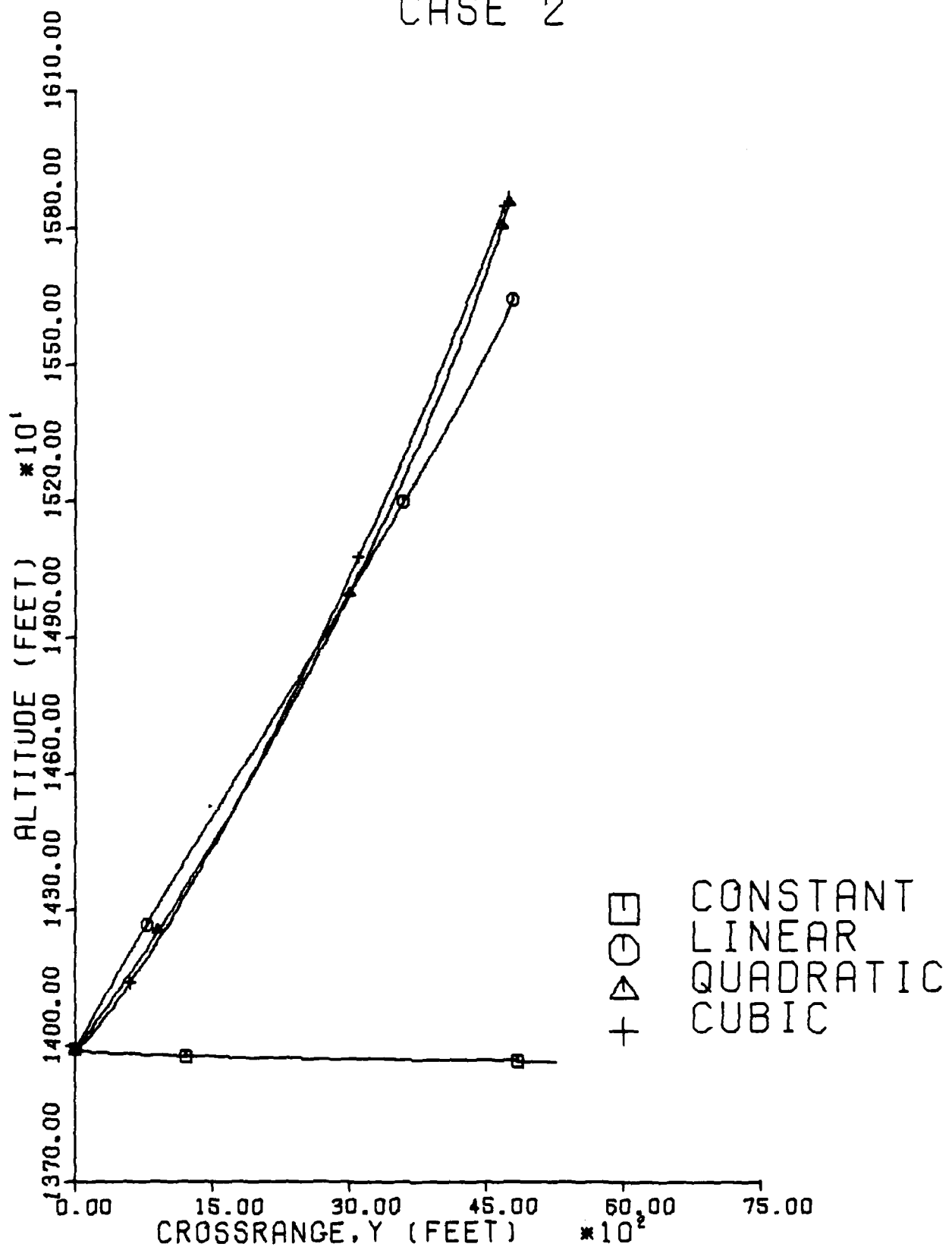


Figure 7. Turn Plane for Case 2 ($V_i=621$ ft/sec, $t=1.10t_{\min}$)

CASE 3

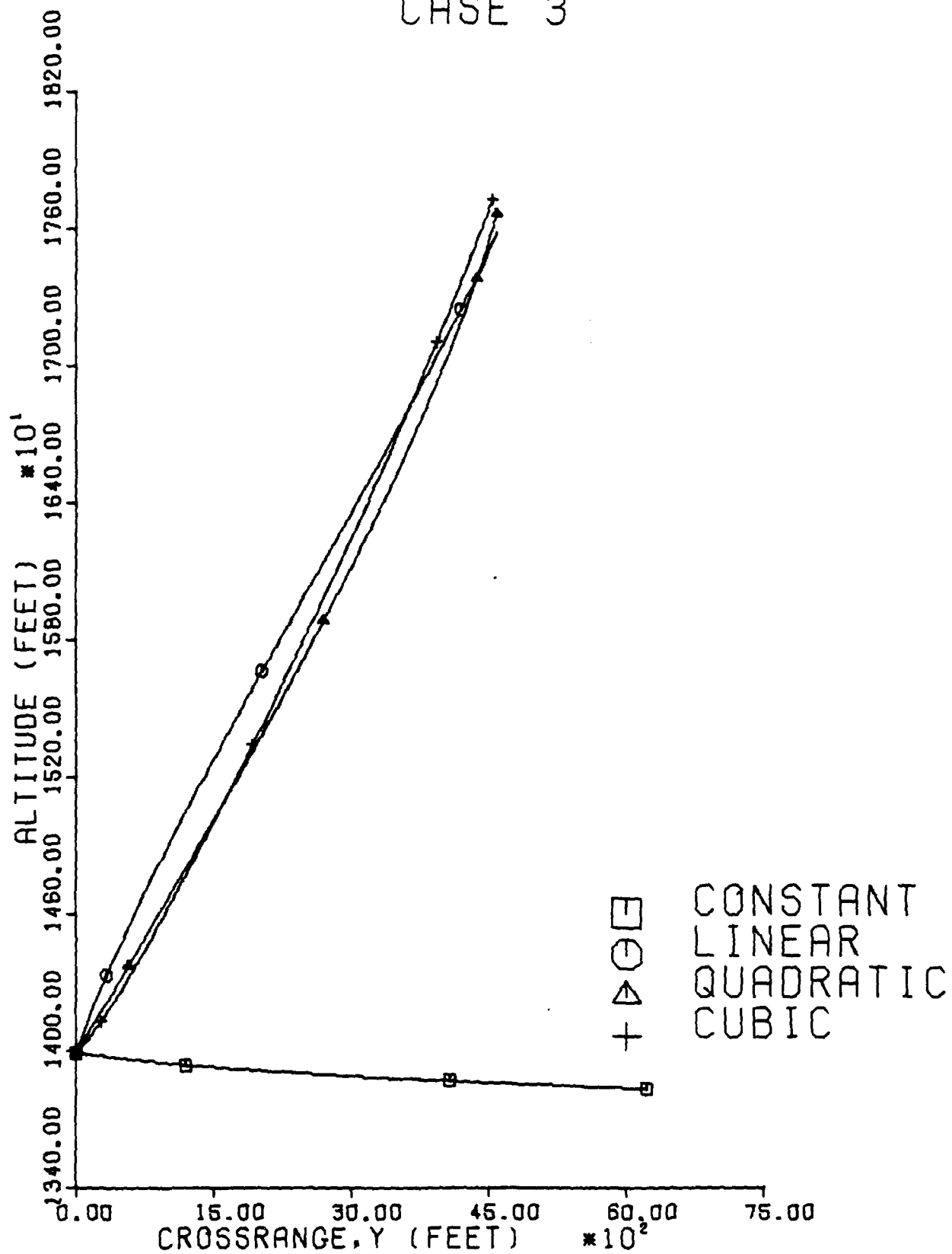


Figure 8. Turn Plane for Case 3 ($V_i=621$ ft/sec, $t=1.25t_{\min}$)

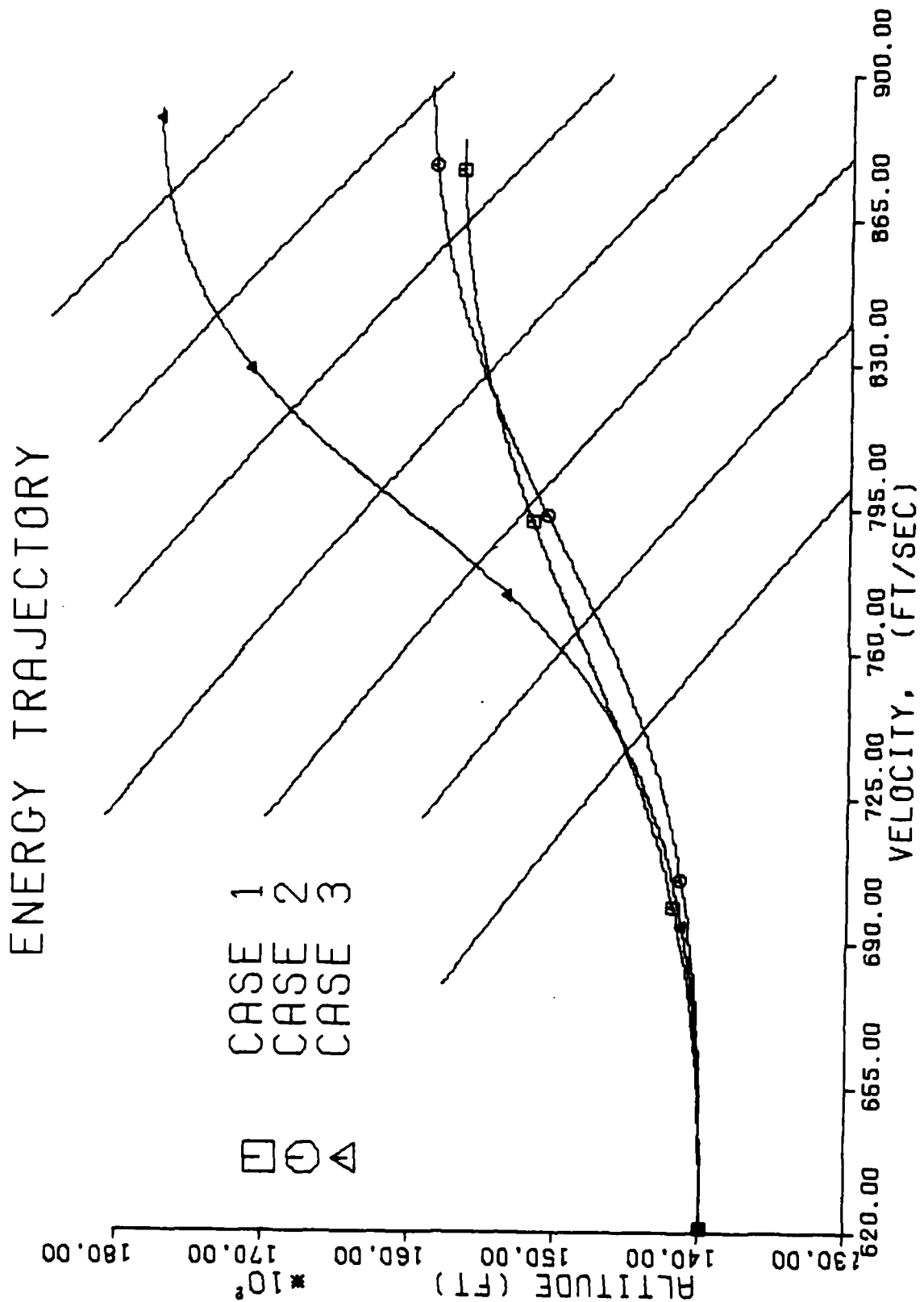


Figure 9. Energy Trajectories for the Low Speed Cases

climb, a minimum time energy trajectory would follow the gradient of the constant energy lines that it crossed. Thus, a velocity-altitude graph would show the trajectory running perpendicular to the constant energy lines. Less efficient trajectories would gain less energy for the same time of flight. In this study, the aircraft climbs higher whenever the turning time is increased. In each successive case the trajectory becomes more perpendicular to the energy lines, hence producing more efficient energy climbs. It is interesting to note that in this study the optimal path is also a perpendicular climb even though the aircraft is also turning as it climbs. Case 3 has a large turning time; it has converged to a perpendicular climb.

The optimal coefficients for cases 4, 5, and 6 are shown in Tables 7, 8, and 9. As before, increasing the bank control complexity increased the performance index. The bank controls were taken up to quintic forms for cases 4 and 5 and a quartic form for case 6. Figure 10 through Fig 12 illustrate the roll controls and Fig 13 through Fig 15 show the turning planes. As the roll control complexity increases, the trajectories become more vertical. Figure 16 shows energy trajectories for these cases. Case 4 loses a lot of velocity as it decelerates toward the corner velocity. As time is increased the energy increases. The trend from case 4 through to case 6 is again to produce a perpendicular climb, though there was insufficient flight time to allow a climb such as

TABLE 7

OPTIMAL COEFFICIENTS FOR CASE 4 ($V_i=903$ ft/sec, $t=1.05t_{\min}$)

	CONSTANT	LINEAR	QUADRATIC	CUBIC	QUARTIC	QUINTIC
FINAL ENERGY	E_f	.300129E+05	.301699E+05	.310458E+05	.312008E+05	.313725E+05
BANK ANGLE COEFF.	B_1	.138384E+01	.144639E+01	.143502E+01	.142231E+01	.141519E+01
	B_2	.134385E+01	.142678E+01	.145746E+01	.150326E+01	.161737E+01
	B_3		.126414E+00	.164823E+00	.106453E+00	.126203E+00
	B_4			-.336684E+00	-.384303E+00	-.352844E+00
	B_5				-.127902E+00	-.139261E+00
	B_6					.139906E+00
THRUST COEFF.	C_1	.572664E+00	.584982E+00	.650098E+00	.662044E+00	.675852E+00
ANGLE OF ATTACK COEFF.	D_1	$\alpha=.2$ if $V < V_C$, $\alpha=(62060.6/V^2)$ if $V > V_C$				
LAGRANGE MULT.	v_1	.297927E+00	.247247E+01	.268197E+01	.264789E+01	.272281E+01
	v_2	-.298275E+01	-.177168E+01	-.160844E+01	-.112913E+01	-.969827E+00

TABLE 8

OPTIMAL COEFFICIENTS FOR CASE 5 ($V_i = 903$ ft/sec, $t = 1.10t_{\min}$)

	CONSTANT	LINEAR	QUADRATIC	CUBIC	QUARTIC	QUINTIC
FINAL ENERGY	E_f					
	.269540E+05	.327849E+05	.329151E+05	.338717E+05	.339975E+05	.342144E+05
BANK ANGLE COEFF.	B_1	.140430E+01	.146371E+01	.145157E+01	.144125E+01	.143616E+01
	B_2	.138988E+01	.145925E+01	.147707E+01	.150810E+01	.163277E+01
	B_3		.113443E+00	.138490E+00	.826552E-01	.103587E+00
	B_4			-.353905E+00	-.394110E+00	-.362107E+00
	B_5				-.110845E+00	-.118101E+00
	B_6					.154551E+00
THRUST COEFF.	C_1	.428269E+00	.797863E+00	.807222E+00	.885971E+00	.914058E+00
ANGLE OF ATTACK COEFF.	D_1	$\alpha = .2$ if $V < V_C$, $\alpha = (62060.6/V^2)$ if $V > V_C$				
LAGRANGE MULT.	v_1	.436976E+00	.248714E+01	.267536E+01	.276705E+01	.287925E+01
	v_2	-.278435E+01	-.162297E+01	-.150435E+01	-.111036E+01	-.857023E+00

TABLE 9

OPTIMAL COEFFICIENTS FOR CASE 6 ($V_i=903$ ft/sec, $t=1.25t_{\min}$)

		CONSTANT	LINEAR	QUADRATIC	CUBIC	QUARTIC
FINAL ENERGY	E_f	.318645E+05	.366623E+05	.366818E+05	.369493E+05	.369547E+05
BANK ANGLE COEFF.	B_1	.143124E+01	.147652E+01	.154591E+01	.152645E+01	.152415E+01
	B_2		.180365E+01	.183776E+01	.174849E+01	.174571E+01
	B_3			.886206E-01	.334844E-01	-.127332E-01
	B_4				-.489936E+00	-.513439E+00
	B_5					-.585983E-01
THRUST COEFF.	C_1	.100000E+01	.100000E+01	.100000E+01	.100000E+01	.100000E+01
ANGLE OF ATTACK COEFF.*	D_1	.969940E-01	.115584E+00	.115702E+00	.113398E+00	.113423E+00
LAGRANGE MULT.	γ_1	.614737E+00	.405321E+00	.433420E+00	.345068E+00	.357167E+00
	γ_2	.621907E-02	-.999758E-01	-.936557E-01	-.480118E-01	-.464793E-01

*: When $V > V_c$, $\alpha = (62060.6/V^2)$.

CASE 4

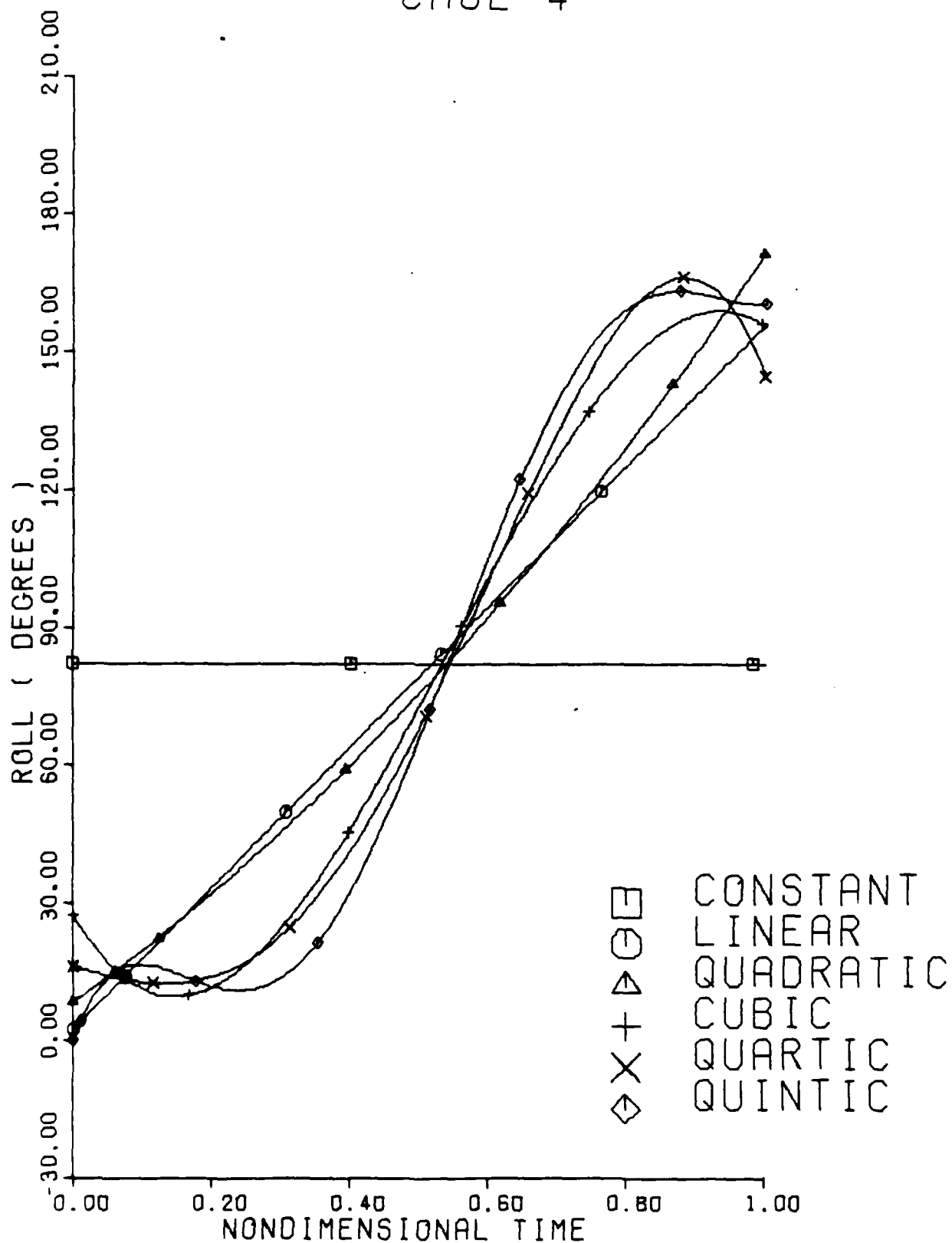


Figure 10. Roll Angle for Case 4 ($V_1=903$ ft/sec, $t=1.05t_{min}$)

CASE 5

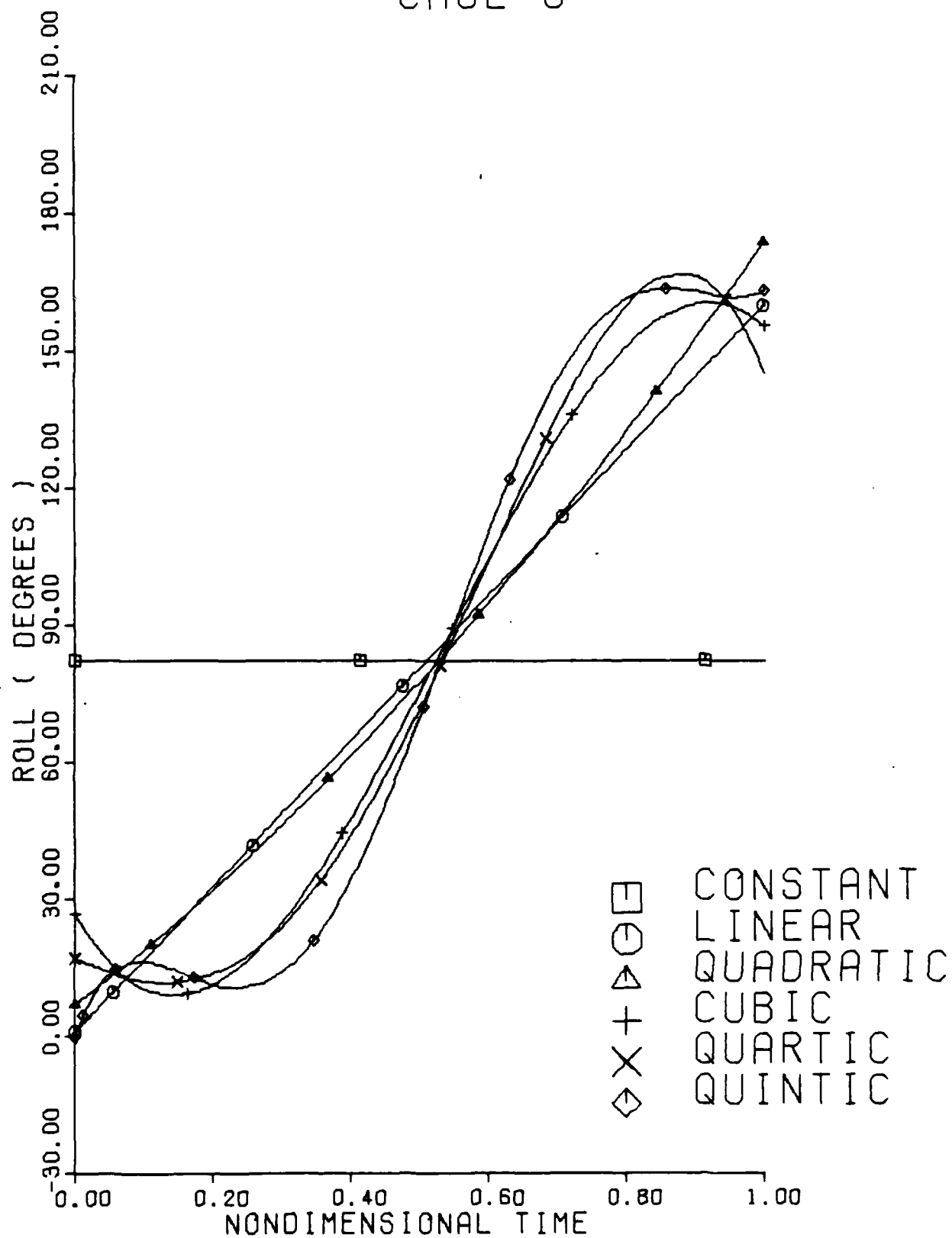


Figure 11. Roll Angle for Case 5 ($V_i=903$ ft/sec, $t=1.10t_{\min}$)

CASE 6

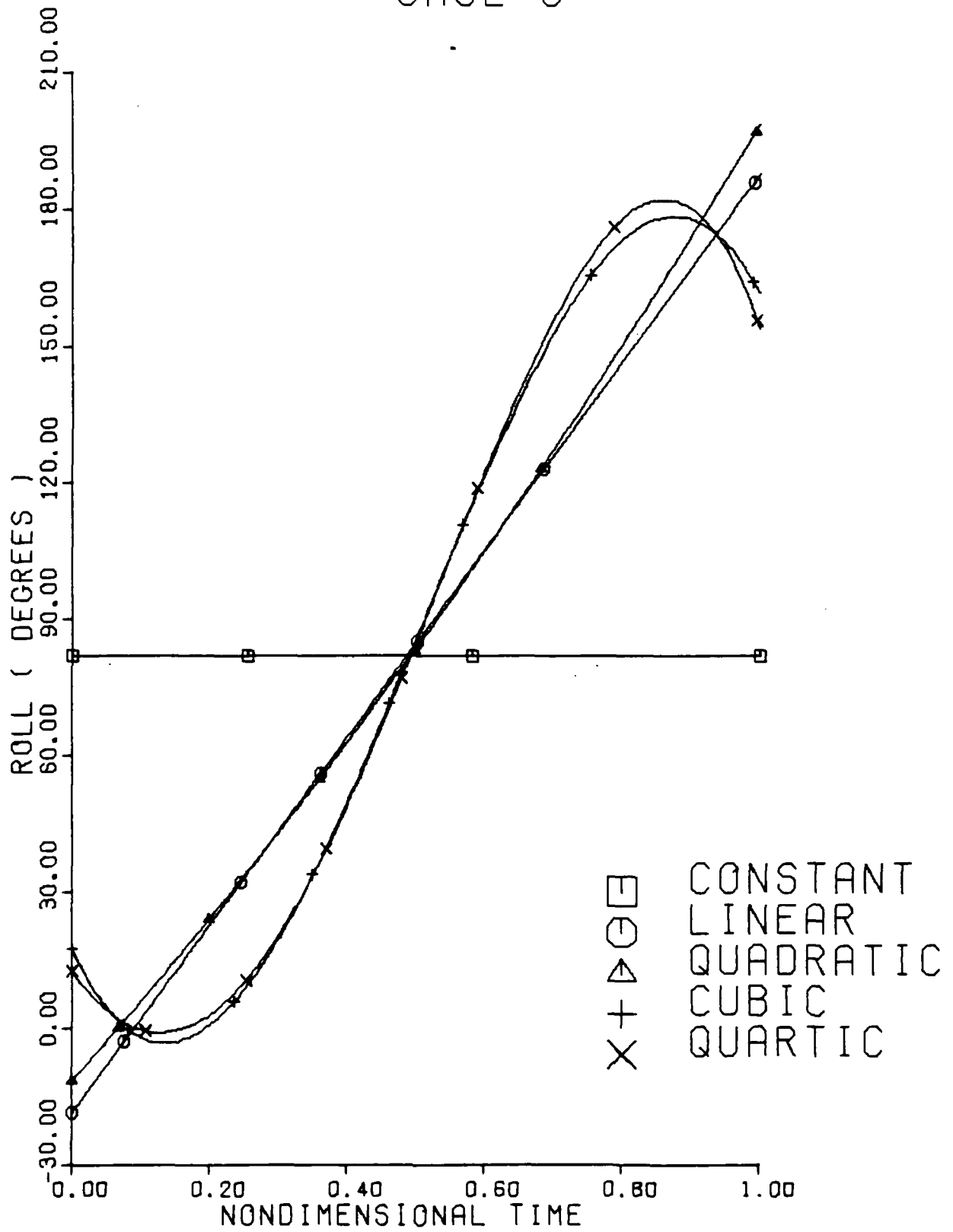


Figure 12. Roll Angle for Case 6 ($V_i=903$ ft/sec, $t=1.25t_{min}$)

CASE 4

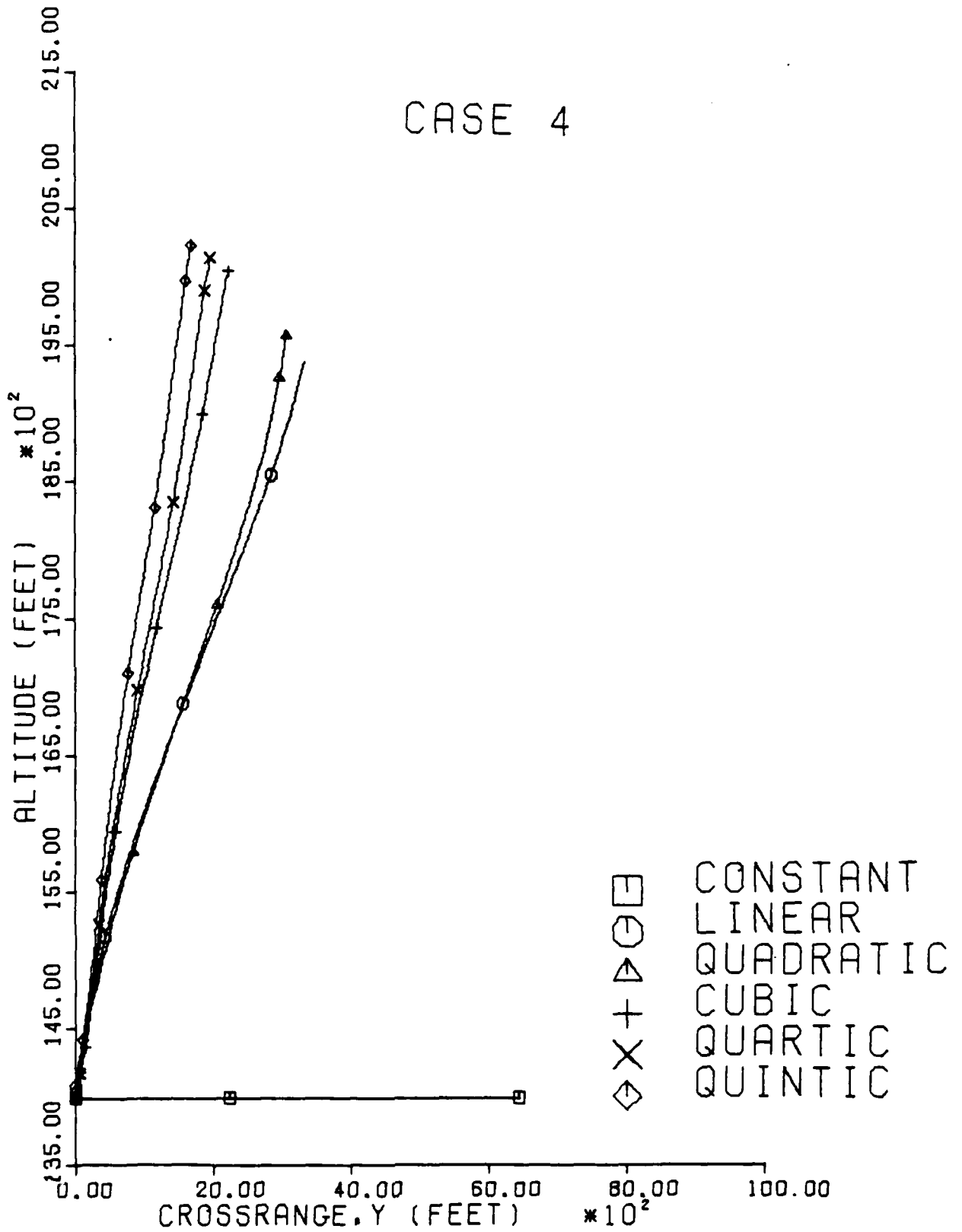


Figure 13. Turn Plane for Case 4 ($V_i=903$ ft/sec, $t=1.05t_{min}$)

CASE 5

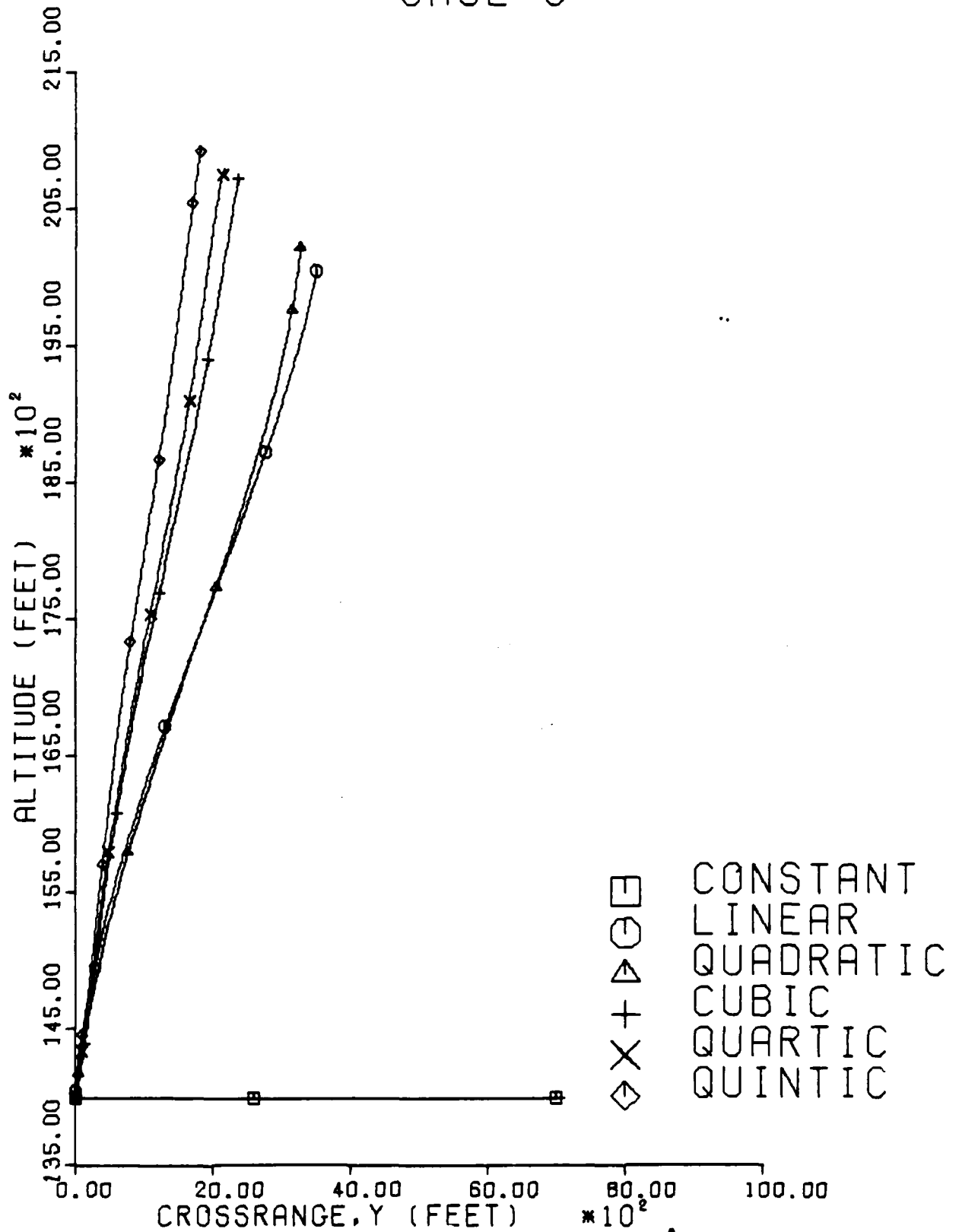


Figure 14. Turn Plane for Case 5 ($V_i=903$ ft/sec, $t=1.10t_{min}$)

CASE 6

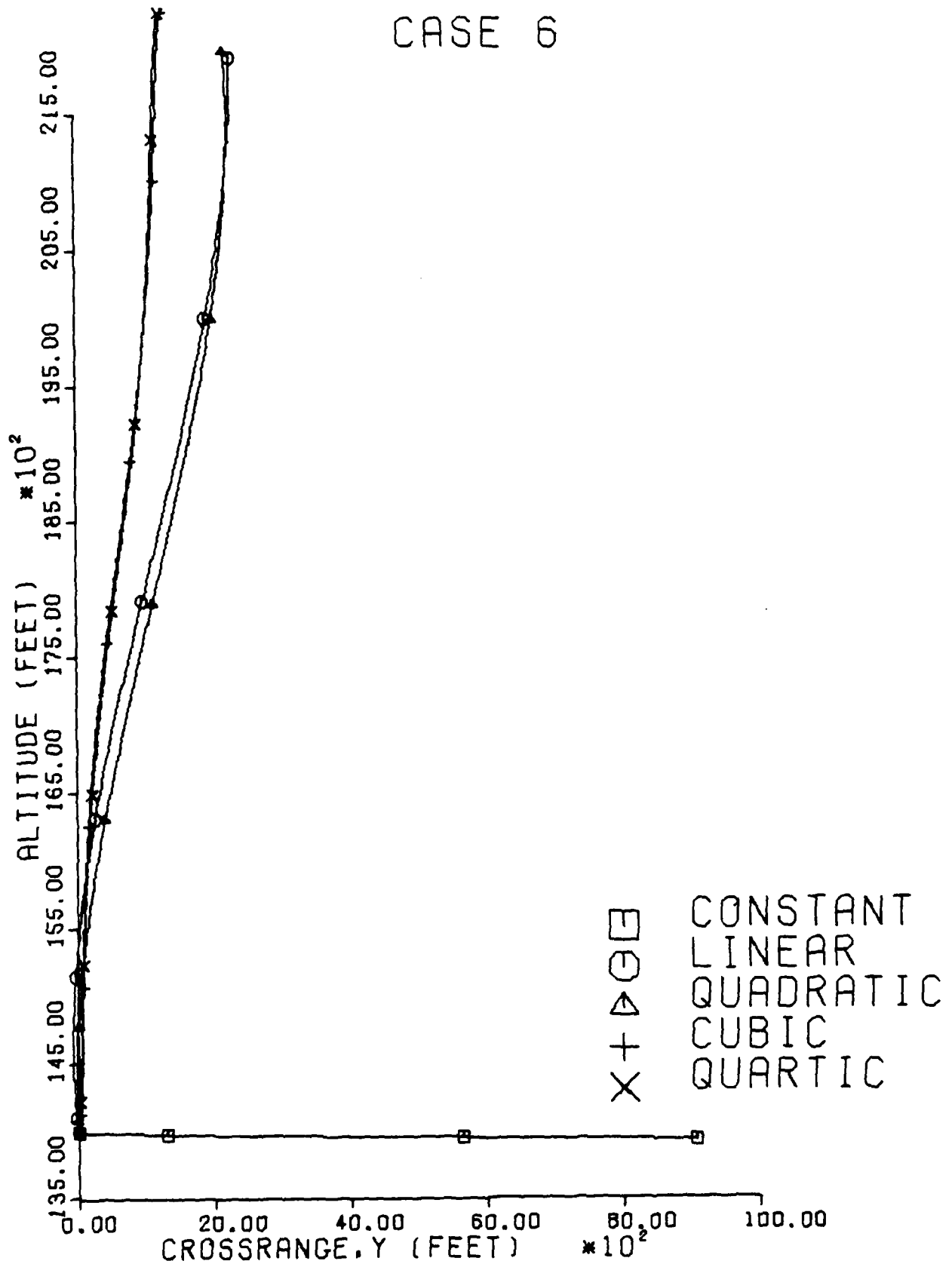


Figure 15. Turn Plane for Case 6 ($V_i = 903$ ft/sec, $t = 1.25t_{\min}$)

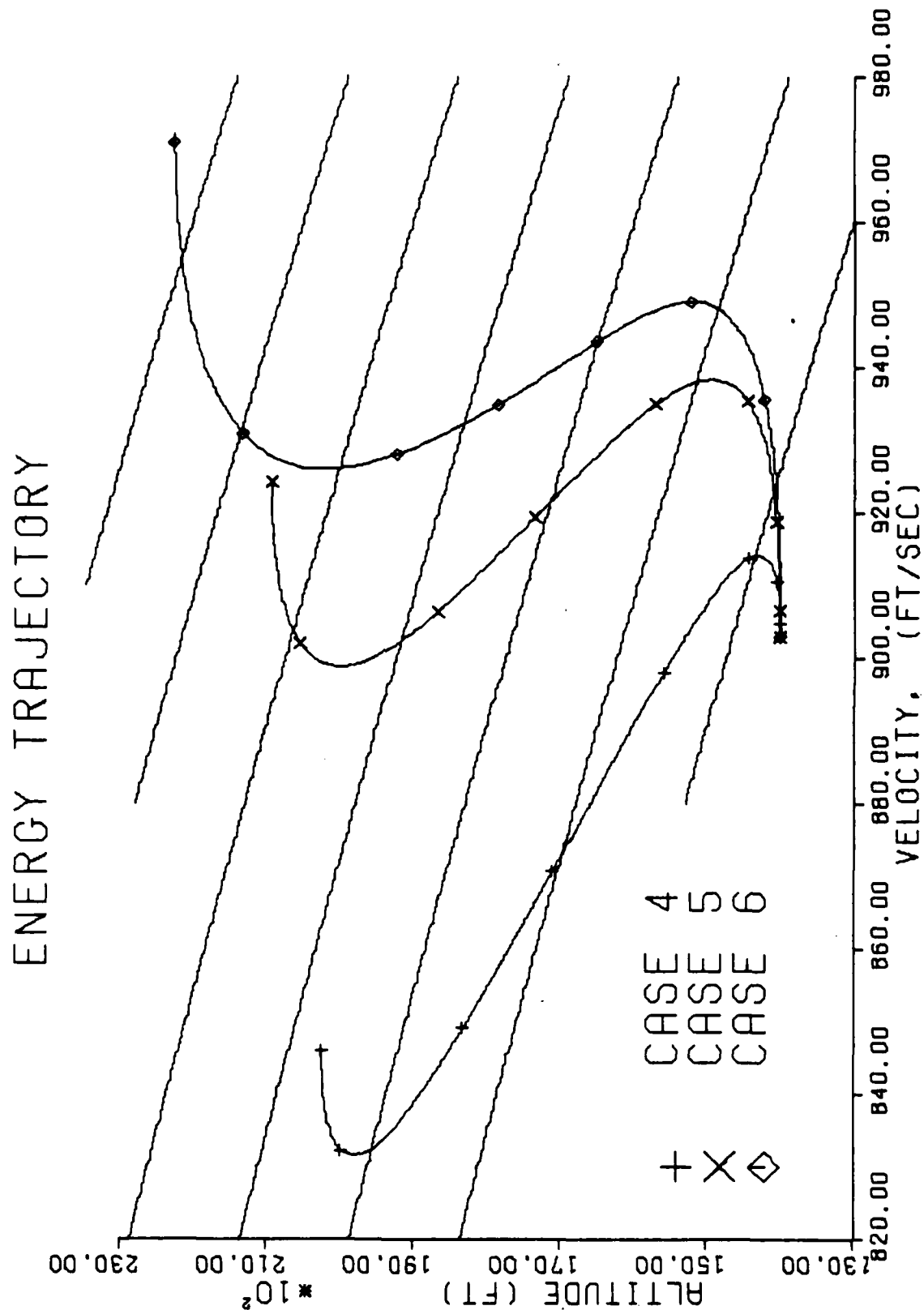


Figure 16. Energy Trajectories for High Speed Cases 4, 5, and 6

case 3. Cases 4, 5, and 6 had a constant angle of attack and throttle, as the first three cases did. Cases 4 and 5 had a partial throttle ($\pi < 1$) which limited the energy available to the aircraft. During any turn the throttle energy can be converted to increased altitude or velocity. In these cases the angle of attack was already at the limit, hence preventing further altitude gain. The turning time limited the turning velocity, hence it could not be increased. The partial throttle values that were computed for these cases represent the maximum energy that could be converted during the turn.

Linear throttle controls were used with the initial conditions and final conditions of cases 4 and 5, creating cases 7 and 8. It was expected that a different throttle control could increase the energy available during the turn. The new throttle controls had a very high slope and crossed both the lower and higher boundaries of the control range. This implied that bang-bang controls would be appropriate. A bang-bang control can instantly switch from off to on, and viceversa. The controls that were computed required off-thrust initially, and then full-thrust after a short time into the turn. Table 10 has the control coefficients for cases 7 and 8 and Fig 17 shows the roll histories. The turning planes are shown in Fig 18. Figure 19 illustrates all the high-speed energy trajectories (cases 4 through 8). Cases 7 and 8 both have more perpendicular trajectories than the comparative cases 4 and 5. Both cases initially decelerate, allowing the aircraft to accomplish a good portion of the turn. Then the aircraft

TABLE 10

OPTIMAL COEFFICIENTS FOR CASES 7 AND 8 ($V_i=903$ ft/sec, $t=1.05t_{\min}$ and $1.10t_{\min}$)

		CASE 7, QUINTIC	CASE 8, QUINTIC
FINAL ENERGY	E_f	.333443E+05	.348133E+05
BANK ANGLE COEFF.	B_1	.144916E+01	.144489E+01
	B_2	.165662E+01	.169280E+01
	B_3	.855829E-01	.949191E-01
	B_4	-.371239E+00	-.385054E+00
	B_5	-.104202E+00	-.113690E+00
	B_6	.169633E+00	.173015E+00
THRUST TURN-ON TIME	C_1	.230280E+01 (sec)	.649602E+00 (sec)
ANGLE OF ATTACK COEFF.	D_1	$\alpha=.2$ if $V \leq V_c$, $\alpha=(62060.6/V^2)$ if $V > V_c$	
LAGRANGE MULT.	v_1	.144079E+01	.105644E+01
	v_2	-.408185E+00	-.264161E+00

BANG-BANG CONTROLS

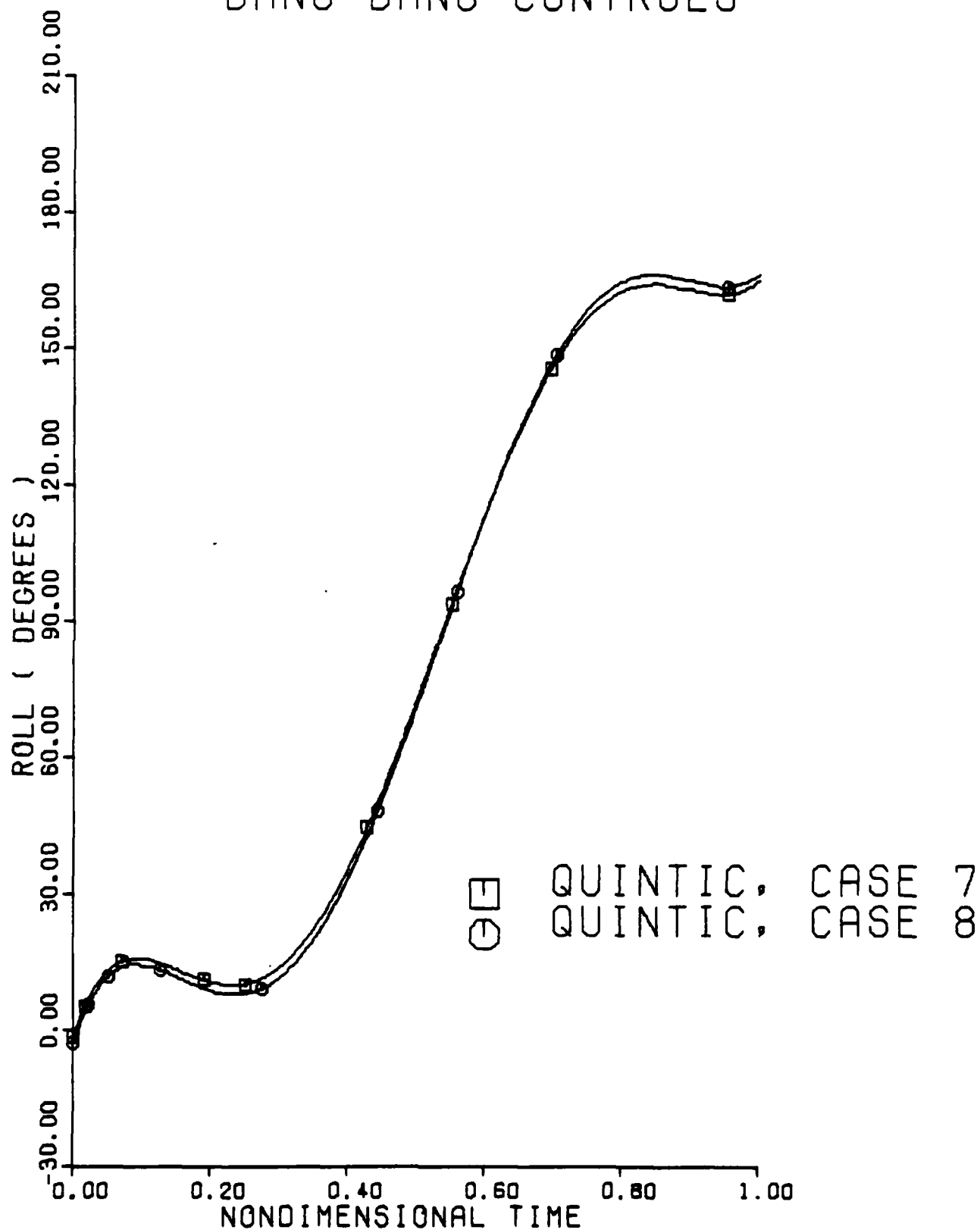


Figure 17. Roll Angle for Case 7 ($V_i=903$ ft/sec, $t=1.05t_{min}$), and Case 8 ($V_i=903$ ft/sec, $t=1.10t_{min}$)

BANG-BANG CONTROLS

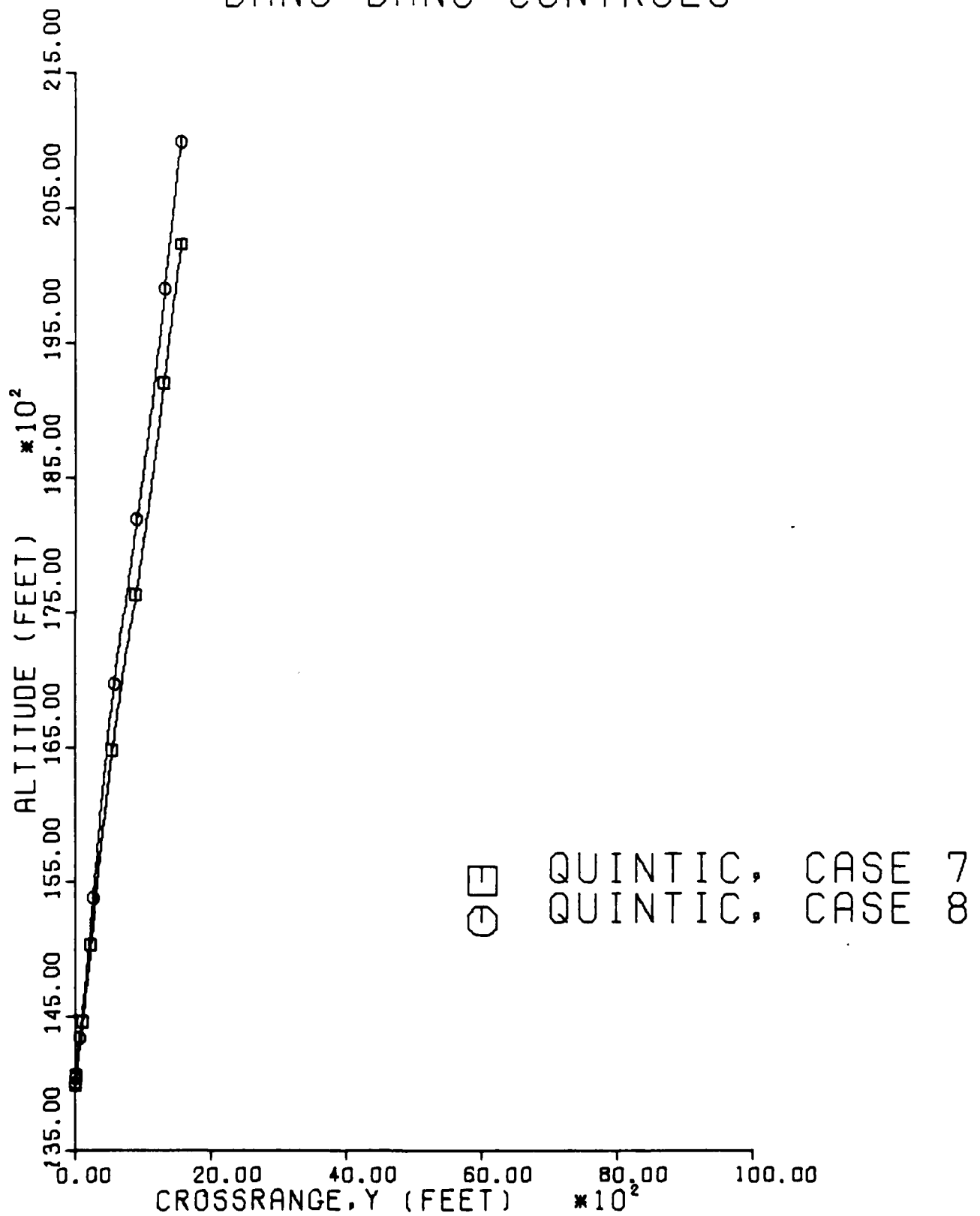


Figure 18. Turn Plane for Case 7 ($V_i=903$ ft/sec, $t=1.05t_{\min}$), and Case 8 ($V_i=903$ ft/sec, $t=1.10t_{\min}$)

ENERGY TRAJECTORY

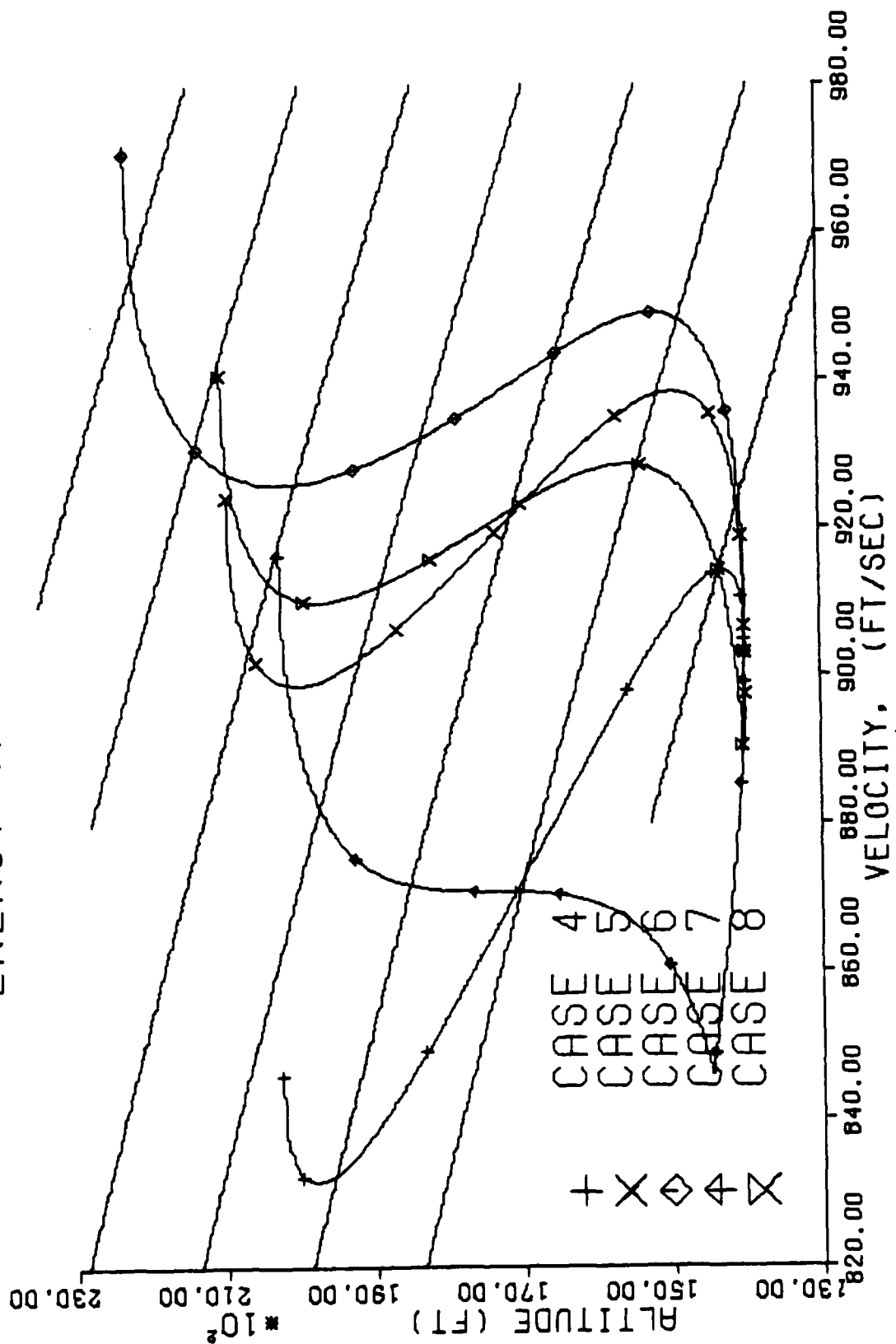


Figure 19. Energy Trajectories for all High Speed Cases

attains a high rate of climb and cuts across the energy lines in an efficient manner.

The energy gains for the final trajectory of every case are shown in Table 11. All the turns have higher energies than the minimum time turns, and the energy always increases as the time increases. The benefit of increased energy would have to be weighed against the increased turning time.

Thrust Reversal

Cases 7 and 8 use bang-bang controls to increase performance over the constant throttle cases. However, this type of throttle control would be impossible to implement with today's engines, since the engines require a few seconds to cycle from idle to full power. One possible way to avoid this problem is to operate the engine at full power and deflect a portion of the thrust. By using a mechanical thrust reverser on the engine nozzle, one could reverse 50% of the thrust and produce zero net thrust. Full thrust would be available with retraction of the reverser, and this could be accomplished very quickly. This would have the additional advantage of eliminating engine thermal cycles, thus improving maintenance.

Pilot Technique

The trajectories obtained here can be generalized to yield a few rules-of-thumb for pilots attempting to fly energy trajectories.

For the low speed cases, throttle should be set at maximum and the load factor held at the maximum throughout the turn. This turn can be improved by adjusting the roll

in order to stay in the same turning plane.

For the high speed cases the angle of attack is held on the angle of attack limit and the throttle should be varied depending on how long the pilot is willing to stay in the turn. A higher throttle increases energy but takes longer to turn. Roll should be used to hold the turn in a plane.

VII Conclusions and Recommendations

The following conclusions and recommendations are based on the results of this study.

The Suboptimal Control Approach is an effective means of solving trajectory problems such as this one. The method is straightforward and offers many advantages over the Optimal Control Approach.

Increasing turning time allows substantial gains in energy. Table 11 shows that even a small increase in time can greatly increase the final energy. For the low speed case, a 5% time increase yields a 29% energy gain over the minimum time result. For the high speed case, a 5% increase will allow a gain of 33% final energy over the minimum time case. This 33% gain amounts to 8701 energy feet. As the times were increased by 10% and 25%, the results were even better for both the high and low speed situations. Bang-bang controls were effective in improving performance for the high speed cases. These controls could possibly be implemented with an in-flight thrust reverser.

Relatively simple techniques can be used to fly energy turns. In most cases a full throttle is permissible, thus freeing the pilot to concentrate on the angle of attack and the roll angle.

It is recommended that vertical climbs be investigated as ways to perform energy turns. These would be Immelman maneuvers. The equations of motion would have to be modified

TABLE 11

ENERGY SUMMARY

	h_i (ft)	V_i (ft/sec)	t (sec)	h_f (ft)	V_f (ft/sec)	E_i (ft)	E_f (ft)	ΔE (ft)	$\Delta E/E_i$ (%)	$\Delta\%$ (%)
LOW SPEED:										
MIN TIME	13990	621	9.643	17338	781	19991	22110	2119	10.6	-
CASE 1	13990	621	10.125	15658	883	19991	27802	7811	39.1	28.5
CASE 2	13990	621	10.607	15877	897	19991	28384	8393	42.0	31.4
CASE 3	13990	621	12.054	17729	890	19991	30067	10076	50.4	39.8
HIGH SPEED:										
MIN TIME	13990	903	11.178	15603	674	26679	22672	-4007	-15.0	-
CASE 4	13990	903	11.737	20233	846	26679	31373	4694	17.6	32.6
CASE 7	13990	903	11.737	20232	918	26679	33344	6665	25.0	40.0
CASE 5	13990	903	12.296	20922	924	26679	34214	7535	28.2	43.2
CASE 8	13990	903	12.296	20922	942	26679	34818	8135	30.5	45.5
CASE 6	13990	903	13.973	22252	972	26679	36955	10276	38.5	53.5

because the $\dot{\psi}$ equation (eqn 13) would have an undefined term at $\theta = 90^\circ$. The crossrange graphs show increasingly vertical lines as the roll coefficients are increased, implying that a vertical climb would be interesting to investigate.

Bibliography

1. Bergman, Dave. "Thrust Vectoring Applied to Aircraft Having High Wing Loading," Aircraft Systems and Technology Meeting: American Institute of Aeronautics and Astronautics, 1979.
2. Brown, David A. "Vectored-Thrust Maneuverability Explored," Aviation Week and Space Technology: 36-39 (December 1971).
3. Linderman, Hoelzer, and Howard. "Test and Evaluation of a Fighter Aircraft In-Flight Thrust Reverser," AIAA Paper 74-1170, AIAA/SAE 10th Propulsion Conference: American Institute of Aeronautics and Astronautics, 1974.
4. Johnson, Thomas. "Minimum Time Turns With Thrust Reversal," Master Thesis, AFIT/GAE/AA/79D-6. Air Force Institute of Technology, Wright Patterson AFB OH, 1979.
5. NASA. U.S. Standard Atmosphere. Washington D.C., December 1962.
6. Humphreys, Hennig, Bolding, and Helgeson. "Optimal 3-Dimensional Minimum Time Turns for an Aircraft," The Journal of the Astronautical Sciences, XX (2): 88-112 (September-October 1972).
7. Hull and Edgeman. "Suboptimal Control Using a Second-Order Parameter-Optimization Method," Journal of Optimization Theory and Application, 17 (5/6): 482-491 (December 1975).
8. Williamson, W.E. "Use of Polynomial Approximations to Calculate Suboptimal Controls," AIAA Journal, (9/11): 2271-2273 (November 1971).
9. Miele, Angelo. "Theory of Flight Paths," Flight Mechanics, 1. Massachusetts: Addison-Wesley Publishing Company, Inc., 1962.
10. Larson, E.W. Lecture materials distributed in AE 6.43, Aircraft Performance. School of Engineering, Air Force Institute of Technology, Wright Patterson AFB OH, 1979.

11. Rader, Captain J. Lecture materials distributed in MC 5.24, Optimization Techniques I. School of Engineering, Air Force Institute of Technology, Wright Patterson AFB OH, 1979.
12. _____. Lecture materials distributed in MC 6.24, Optimization Techniques II. School of Engineering, Air Force Institute of Technology, Wright Patterson AFB OH, 1979.
13. Fehlberg, Erwin. Classical Fifth-, Sixth-, Seventh-, and Eighth- Order Runge-Kutta Formulas with Stepsize Control. NASA-TR-R-287. Washington D.C., NASA, 1968.
14. Hornbeck, Robert W. Numerical Methods. New York: Quantum Publishers, Inc., 1975.
15. Rutowski, Edward S. "Energy Approach to the General Aircraft Performance Problem," Journal of the Aeronautical Sciences: 187-195 (March 1954).

VITA

Steven Petersen was born 19 May 1955 in Oak Park, Illinois. He graduated from high school in Wilmette, Illinois, in 1973 and attended the United States Air Force Academy in Colorado Springs, Colo. He received a Bachelor of Science degree in Engineering Science in 1977 and received a regular commission in the USAF. He was assigned to the Test Engineering Division of the 6594th Test Group at Hickam AFB HI, and spent two years there. During this time he worked as a Space Systems Recovery Engineer. He entered the School of Engineering, Air Force Institute of Technology in June, 1979.

Permanent address: 120 N. Lake Shore Dr. #937
N.Palm Beach, Florida 33408

UNCLASSIFIED

SECURITY CLASSIFICATION OF THIS PAGE (When Data Entered)

REPORT DOCUMENTATION PAGE		READ INSTRUCTIONS BEFORE COMPLETING FORM
1. REPORT NUMBER AFIT/GAE/AA/80D-17	2. GOVT ACCESSION NO. AD-A094733	3. RECIPIENT'S CATALOG NUMBER
4. TITLE (and Subtitle) TIME-CONSTRAINED MAXIMUM-ENERGY TURNS		5. TYPE OF REPORT & PERIOD COVERED MS Thesis
		6. PERFORMING ORG. REPORT NUMBER
7. AUTHOR(s) Steven Petersen 1st Lt. USAF		8. CONTRACT OR GRANT NUMBER(s)
9. PERFORMING ORGANIZATION NAME AND ADDRESS Air Force Institute of Technology (AFIT/ENA) Wright-Patterson AFB OH 45433		10. PROGRAM ELEMENT, PROJECT, TASK AREA & WORK UNIT NUMBERS
11. CONTROLLING OFFICE NAME AND ADDRESS		12. REPORT DATE December 1980
		13. NUMBER OF PAGES 71
14. MONITORING AGENCY NAME & ADDRESS (if different from Controlling Office)		15. SECURITY CLASS. (of this report)
		15a. DECLASSIFICATION DOWNGRADING SCHEDULE
16. DISTRIBUTION STATEMENT (of this Report) Approved for public release; distribution unlimited.		
17. DISTRIBUTION STATEMENT (of the abstract entered in Block 20, if different from Report) Approved for public release; IAW AFR 190-17 FREDRIC C. LYNCH, Major, USAF 30 DEC 1980 Director of Public Relations		
18. SUPPLEMENTARY NOTES		
19. KEY WORDS (Continue on reverse side if necessary and identify by block number) Energy Optimization Performance Control		
20. ABSTRACT (Continue on reverse side if necessary and identify by block number) The object of this study is to find the trajectories which a high performance aircraft would employ to maximize the change in specific energy during a prescribed turn. These values of the change in specific energy are compared to the changes in specific energy which result from a minimum time turn. A suboptimal control approach, which uses both gradient and second-order techniques, is employed to find the maximum specific energy trajectories. The		

DD FORM 1473

EDITION OF 1 NOV 65 IS OBSOLETE

UNCLASSIFIED

SECURITY CLASSIFICATION OF THIS PAGE (When Data Entered)

UNCLASSIFIED

SECURITY CLASSIFICATION OF THIS PAGE(When Data Entered)

→ results of the study show that turning times slightly greater than the minimum turning time allow large increases in aircraft specific energy, and that the trajectories can be flown with simple control inputs. ←

B

UNCLASSIFIED

SECURITY CLASSIFICATION OF THIS PAGE(When Data Entered)

FILMED
— 8